ORGANOMETALLICS

Article

pubs.acs.org/Organometallics

New Aryl α-Diimine Palladium(II) Catalysts in Stereocontrolled CO/Vinyl Arene Copolymerization

Carla Carfagna,*[,†] Giuseppe Gatti,[†] Paola Paoli,[‡] Barbara Binotti,[†] Francesco Fini,[†] Alessandra Passeri,[†] Patrizia Rossi,[‡] and Bartolo Gabriele[§]

[†]Dipartimento di Scienze Biomolecolari, Università di Urbino "Carlo Bo", Piazza Rinascimento 6, 61029 Urbino, Italy

[‡]Dipartimento di Ingegneria Industriale, Università di Firenze, Via S. Marta 3, 50139 Firenze, Italy

[§]Dipartimento di Chimica e Tecnologie Chimiche, Università della Calabria, Via P. Bucci, 12/C, 87036 Arcavacata di Rende (CS), Italy

Supporting Information

ABSTRACT: The effect of the catalyst structure on the stereoselectivity of CO/vinyl arene copolymerization has been studied with the aim of developing catalytic systems able to improve the yields while maintaining the high degree of copolymer isotacticity previously obtained using achiral nitrogen ligands. Aryl α-diimine ligands having extended aromatic rings $(Ar)_2DABMe_2$, with Ar = 1-$C_{10}H_7$ (**e**), 1-$C_{14}H_9$ (**f**), 9-$C_{14}H_9$ (**g**), have been synthesized, and α-diimine coordination to cationic methylpalladium complexes has been investigated in solution, by means of NMR spectroscopy, and in the solid state for [Pd(Me)(NCMe)((9-$C_{14}H_9)_2$DABMe$_2$)][PF_6] (**2g**). The performance of these catalysts in CO/vinyl arene copolymerization, under mild conditions, was analyzed in terms of productivity and degree of stereoregularity of the resulting polyketones. In comparison with previous results, a remarkable enhancement in the yield of isotactic copolymer was observed using the new achiral 9-anthryl α-diimine ligand **g**, confirming that the ortho disubstitution and the extended aromatic rings play key roles in obtaining good stereoselectivity and good productivity. To perform a structural analysis of the first steps of the CO/*p*-methylstyrene copolymerization, complex [Pd(Me)(CO)((9-$C_{14}H_9)_2$DABMe$_2$)][BAr′$_4$] (**3g**) was used as a starting point: NMR investigation reveals the stereoselective formation of the olefin/CO/olefin insertion product (**6g**), which prevalently exists in solution in only one diastereoisomeric form, thus justifying the observed high polymer isotacticity.

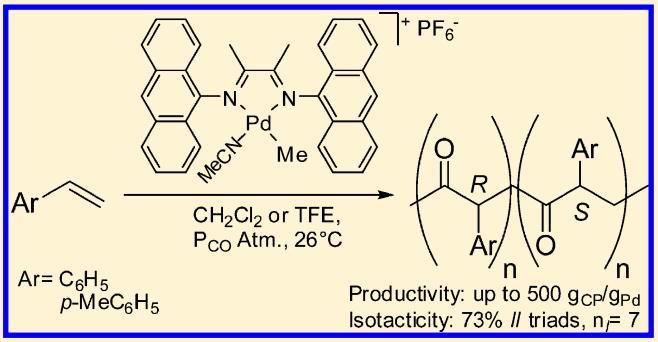

1. INTRODUCTION

Late-transition-metal catalysts bearing nitrogen ligands have found applications in several polymerization reactions. Within these numerous kinds of complexes, palladium(II) catalysts containing ortho-substituted aryl diimines appear to be rather peculiar. Depending on the steric hindrance of the ortho substituents, they are excellent catalysts for homopolymerization of olefins[1] or quite good catalysts for the alternating copolymerization of aromatic olefins with carbon monoxide.[2] The latter is one of the best ways to efficiently synthesize polar functionalized polymers through a coordination−insertion mechanism.[3] The resulting polyketone possesses valuable properties: mechanical and surface characteristics can be easily tuned, and the polymer chain can be postfunctionalized, due to the presence of the carbonyl group.[4] These characteristics, together with the promising biocompatibility of produced materials,[5] make the CO/olefin copolymerization still an attractive research field.[6] Nevertheless, few examples of this process, using α-diimine catalysts, have been reported.[2] The key role played by the aryl-substituted α-diimine structure on the reactivity of the metal complex is well-known. In olefin polymerization, the presence of bulky nitrogen ligands is crucial for blocking the axial coordination sites on the metal toward incoming monomer, retarding the chain transfer.[1] Conversely, in CO/olefin copolymerization the presence of large ortho substituents on the aryl rings[7] is critical in determining the stereoselectivity of the Pd(II) catalysts,[2b−d] as observed by some of us during recent investigations on CO/vinyl arene copolymerization catalyzed by the complexes [Pd(η^1,η^2-C_8H_{12}OMe)($(Ar)_2DABR_2$)]X and [Pd(Me)(NCMe)($(Ar)_2DABR_2$)]X bearing achiral α-diimine ligands ($(Ar)_2DABR_2$ ≡ ArN═C(R)C(R)═NAr).[2a−c,8] These catalysts are able to produce atactic or stereoblock isotactic CO/*p*-methylstyrene copolymers, depending on the aryl substituents, through a "ligand assisted" chain-end control mechanism: both the ligand and the growing chain cooperate in selecting the enantioface and the direction of the incoming olefin during the copolymerization process.[2d,8] This behavior is different from that observed with other achiral ligands (C_{2v} or C_s symmetry), which generally produce highly syndiotactic polyketones due to

Received: September 4, 2013

   dx.doi.org/10.1021/om400887x | *Organometallics* XXXX, XXX, XXX−XXX

chain-end control,[9] while isotactic microstructures are commonly obtained with optically active C_2-symmetric ligands that provide an enantiomorphic site-control propagation.[10] The isotacticity strongly increases using bulky groups in the phenyl ortho positions and in the ligand backbone. From a DFT study it appears that the strong steric interactions between the substituents of the backbone and those in the phenyl ortho positions constrain the phenyl rings to arrange almost perpendicularly with respect to the palladium mean coordination plane and parallel to each other.[8] Reasonably, this affects the coordination of the aromatic olefin and the stereochemistry of the resulting intermediate, inducing high enantioface discrimination and the consequent synthesis of isotactic copolymer. Unfortunately, moderate productivities are generally observed, due to the crowded coordination sites of the catalysts as well as to the low catalyst stability in the copolymerization medium. For example, the complex with the methyl substituents in phenyl ortho positions and in the ligand backbone (i.e., bearing the $(2,6\text{-Me}_2\text{Ph})_2\text{DABMe}_2$ ligand) gives a copolymer characterized by a high degree of isotacticity (*ll* = 74%) but with a modest productivity (about 0.7 (g of CP) (g of Pd)$^{-1}$ h^{-1}) in comparison with that of the atactic copolymer obtained using the $(4\text{-MeOPh})_2\text{DABMe}_2$ ligand (about 4 (g of CP) (g of Pd)$^{-1}$ h^{-1}).[2d] With the main intention of improving the performance of stereoselective CO/vinyl arene copolymerization, our approach was to synthesize complexes in which the structure of the nitrogen ligand, especially its ability to shield the axial positions, allows the production of a stereoregular isotactic polymer without suppressing the catalyst activity. Ligands **e**–**g**, having two or three fused aromatic rings, were synthesized and the catalytic properties of the corresponding novel catalysts **2e**–**g** were tested and compared with those of complexes **2a**–**d** (Scheme 1). Structural analysis was performed

Scheme 1. Synthesis of Complexes 2a–g from 1a–g

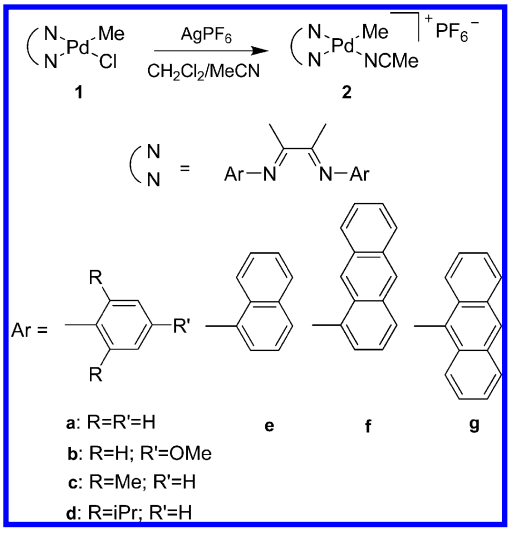

for all compounds, as well as for the first intermediates of the stereoselective CO/*p*-methylstyrene copolymerization catalyzed by complex **2g**.

2. RESULTS AND DISCUSSION

2.1. Synthesis and Characterization of Ligands f and g and Complexes 1e–g and 2a–g. Ligands $(1\text{-}C_{14}H_9)_2\text{DABMe}_2$ (**f**) and $(9\text{-}C_{14}H_9)_2\text{DABMe}_2$ (**g**) were synthesized by condensation of 2,3-butanedione with $(1\text{-}C_{14}H_9)NH_2$ and $(9\text{-}C_{14}H_9)NH_2$, respectively; meanwhile ligand **e** was synthesized according to literature methods.[11] Recently the synthesis of a series of α-diimine ligands with substituted naphthyl groups has been reported.[12] Palladium(II) complexes **1e–g** were obtained from the reaction of [Pd(Me)(Cl)(COD)] (COD = 1,5-cyclooctadiene) with the α-diimine ligands **e**–**g**, in dichloromethane at 25 °C (Scheme 1); the diene was substituted quantitatively by the nitrogen ligand within a few hours. Complexes **1a–g** react with $AgPF_6$ at 0 °C in a CH_2Cl_2/MeCN (5/1, v/v) mixture, leading to the cationic acetonitrile compounds **2a–g** with satisfactory to excellent yield (60–98%) (Scheme 1). Structures of all compounds were investigated in CD_2Cl_2 or $CDCl_3$ by ^{1}H and ^{13}C NMR spectroscopy. The assignments of the ^{1}H and ^{13}C resonances were performed by following the scalar and dipolar nuclear interactions in the ^{1}H–COSY, ^{1}H,^{13}C-HSQC, ^{1}H,^{13}C-HMBC, and ^{1}H-NOESY spectra (data are reported in the Experimental Section).

The comparative analysis of the chemical shifts of the Pd–Me protons in complexes **1a–g** and **2a–g** suggests that the shielding effect exerted by the π electrons of the 9-anthracenediimine ligand in **1g** and **2g** is more important than that of the other ligands (Table 1).

Table 1. Chemical Shift Values ($CDCl_3$, 19 °C) of the Pd–Me Resonance in Complexes Pd(Me)Cl($(Ar)_2$DABMe$_2$) (1a–g) and [Pd(Me)(NCMe)($(Ar)_2$DABMe$_2$)]$^+$[PF_6]$^-$ (2a–g)

Ar	complex **1a–g**	δ (ppm)	complex **2a–g**	δ (ppm)
Ph	**1a**	0.63	**2a**	0.41
4-MeOPh	**1b**	0.65	**2b**	0.47
2,6-Me_2Ph	**1c**	0.44	**2c**	0.29
2,6-*i*Pr_2Ph	**1d**	0.36	**2d**	0.42
1-$C_{10}H_7$	**1e**	0.46	**2e**	0.18, 0.19[a]
1-$C_{14}H_9$	**1f**	0.31	**2f**	0.07, 0.12[a]
9-$C_{14}H_9$	**1g**	0.05	**2g**	−0.03

[a]Two resonances are detected due to the presence in solution of two conformational isomers (vide infra).

A plausible explanation could be found in the larger size of the aromatic portion of ligand **g**, in comparison to **a**–**e**, and in the symmetric placement of the aromatic rings above and below the coordination plane in complexes **1g** and **2g**, differently from what occurs in **1e,f** and **2e,f**. The almost perpendicular orientation of the aromatic rings with respect to the coordination plane (see the X-ray structure of **2g**; Figure 2) favors the observed upfield shift. For complexes **1e,f** and **2e,f**, the NMR investigations indicated that the two possible conformational diastereoisomers in which the nitrogen ligand adopts a C_2- or a C_s-symmetric coordination geometry (Scheme 2: *a* and *b*, C_2-conformational enantiomers; *c* and *d*, C_s-conformational enantiomers), are simultaneously present in CD_2Cl_2 (and $CDCl_3$) solution at 19 °C, with an approximate equimolar ratio. This finding agrees well with previously reported theoretical results for the [$PdCl_2$(Ar-BIAN)] complex[13] (Ar-BIAN = bis(1-naphthylimino)acenaphthene), where the syn and anti isomers are almost isoenergetic. Besides *ab initio* calculations performed on the **e** and **f** nitrogen ligands (Scheme 1) show that the syn and anti conformers differ by a maximum of ca. 1 kcal mol^{-1}, the anti isomer being more stable than the corresponding syn isomer, as expected.[12,13]

The presence (in solution) of both C_2 and C_s conformational isomers generates split signals in both the ^{1}H and ^{13}C NMR

dx.doi.org/10.1021/om400887x | *Organometallics* XXXX, XXX, XXX–XXX

Scheme 2. C_2 and C_s Conformational Isomers of Complex 2e

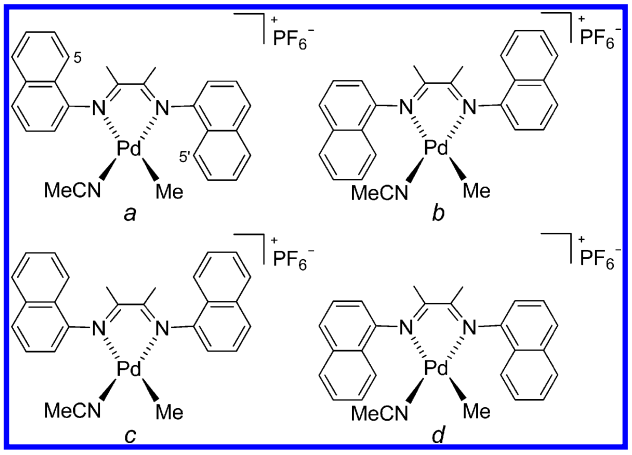

spectra of complexes **1e,f** and **2e,f**. For instance, two defined doublets for the H5 resonance are present in the ^{1}H spectrum of **2e**, centered at 8.25 and 8.17 ppm ($CDCl_3$, 19 °C, $^2J_{HH}$ = 8.2 Hz), corresponding to two carbon signals at 123.8 and 123.4 ppm. Analogously, two singlets are observed at 0.18 and 0.19 ppm attributable to the Pd−Me protons of the two isomers, which correspond to two ^{13}C resonances at 4.43 and 4.37 ppm. Unfortunately, the overlapping of many resonances precludes the unambiguous assignment of all signals.

2.2. CO/Vinyl Arene Copolymerization. Complexes **2a−g** were tested as catalysts in the copolymerization of CO with *p*-methylstyrene (Table 2) or styrene (Table 4); reactions were carried out for 27 h at room temperature (26 °C), under 1 atm pressure of CO, in dichloromethane or TFE (TFE = 2,2,2-trifluoroethanol) (Scheme 3, Tables 2 and 4).

Scheme 3. Copolymerization Reaction

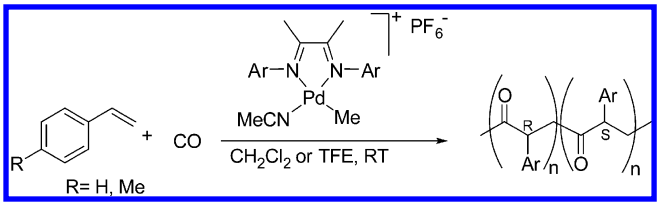

From Table 2 it appears that in CH_2Cl_2 the productivity in CO/*p*-methylstyrene copolymer tends to diminish with an increase in the size of the substituents in the ortho positions of the aromatic rings of the ligand, in fact passing from catalysts **2a,b**, in which the productivity is around 100 (g of CP) (g of Pd)$^{-1}$ (Table 2, entries 1 and 2), to the hemihindered **2e,f** (83 and 58 (g of CP) (g of Pd)$^{-1}$; Table 2, entries 7 and 9) and the hindered **2c,d** (52 and 0 (g of CP) (g of Pd)$^{-1}$; Table 2, entries 3 and 6), a reduction in yields was observed. The only catalyst that does not follow this trend is **2g**, which, although it has encumbered apical positions, is the most active, producing 130 (g of CP) (g of Pd)$^{-1}$ (Table 2, entry 10). An increase in CO pressure up to 5 bar results in a decrease of productivity together with a significant increase of M_w (weight-average molecular weight) (Table 2, entry 10 vs entry 12). Formation of inactive palladium metal was generally observed at the end of the reaction (**2a−c,f**); meanwhile, with catalyst **2e** it was possible to prolong the reaction time up to 51 h, obtaining a yield of 296 (g of CP) (g of Pd)$^{-1}$ (Table 2, entry 8). With styrene as comonomer instead of *p*-methylstyrene an increase in yield and M_w was achieved (see Table 4, entry 1, vs Table 2, entry 10). In addition, considering that the capacity of the TFE as solvent and BQ (1,4-benzoquinone) as oxidant was previously observed to increase the yield of the CO/styrene copolymerization catalyzed by analogous Pd complexes,[2f] reactions with catalysts **2c,e−g** were also carried out in TFE plus BQ. A beneficial effect was observed in all cases, and mainly isotactic copolymer (vide infra) was produced. In particular with catalysts **2g,c** the yield in *p*-methylstyrene/CO copolymer was more than doubled in TFE and BQ in comparison to that in methylene chloride (Table 2, entry 10 vs entry 11 and entry 3 vs entry 5). Combining the use of styrene as comonomer and TFE as solvent plus BQ, a sharp increase in productivity was recorded with catalysts **2e−g**, giving up to 564 (g of CP) (g of Pd)$^{-1}$ (Table 4, entry 3). In agreement with the literature, the productivity is affected by four main factors: the structure of the nitrogen ligand and therefore of the catalyst, the kind of olefin comonomer, the nature of the reaction solvent, and the presence of the oxidant.

The influence of the catalyst structure on the productivity ((g of CP) (g of Pd)$^{-1}$) is evident from the trend found in

Table 2. CO/*p*-Methylstyrene Copolymerization Results[a]

					triad (%)[c]				
entry	cat.	yield (g)[b]	CP (%)	productivity ((g of CP) (g of Pd)$^{-1}$)	*ll*	*ul/lu*	*uu*	n_l	$10^{-3}M_w$ (PDI)[d]
1	**2a**	0.480	78	101	30	49	21	2.2	7.5 (1.9)
2	**2b**	0.450	94	114	25	53	22	2.0	10.5 (1.8)
3	**2c**	0.200	96	52	71	26	3	6.5	9.2 (1.3)
4[e]	**2c**	0.355	96	91	69	29	2	5.8	15.4 (1.2)
5[f]	**2c**	0.535	87	125	71	26	3	6.5	6.6 (1.6)
6	**2d**	0.096	<1						
7	**2e**	0.448	69	83	53	37	10	3.9	4.4 (1.6)
8[g]	**2e**	1.160	95	296	51	41	8	3.5	18.0 (3.2)
9	**2f**	0.221	97	58	45	44	11	3.1	10.5 (1.4)
10	**2g**	0.495	>99	130	71	25	4	6.7	16.7 (1.2)
11[f]	**2g**	1.080	>99	290	72	25	3	6.8	8.5 (1.6)
12[h]	**2g**	0.608	60	98	73	23	4	7.4	27.6 (1.8)

[a]Reaction conditions: n_{Pd} = 0.035 mmol; volume of *p*-methylstyrene 2.8 mL (21 mmol, Pd/olefin = 1/600); solvent CH_2Cl_2 (2.8 mL); T = 26 °C; P_{CO} = 1 atm; t = 27 h. [b]Total yield of homopolymer (HP) and copolymer (CP). [c]Evaluated from the intensities of the ^{13}C NMR ipso carbon atom resonances. [d]PDI = M_w/M_n. [e]Solvent 2,2,2-trifluoroethanol. [f]Solvent 2,2,2-trifluoroethanol (2.8 mL); Pd/1,4-benzoquinone = 1/5. [g]t = 51 h. [h]P_{CO} = 5 atm.

dx.doi.org/10.1021/om400887x | *Organometallics* XXXX, XXX, XXX−XXX

CH_2Cl_2: **2g** (130) > **2b** (114) > **2a** (101) > **2e** (83) > **2f** (58) > **2c** (52) > **2d** (0) (Table 2, entries 10, 2, 1, 7, 9, 3, and 6, respectively), which seems related to the pK_a values of the anilines employed in the synthesis of the corresponding ligands (except for **2d**) (Table 3).[14]

Table 3. Relationship between the pK_a Values of the Anilines and the Productivities of the Corresponding Complexes 2a−g

entry	aniline	pK_a	cat.	productivity ((g of CP) (g of Pd)$^{-1}$)
1	9-$C_{14}H_9NH_2$	6.34[15a]	**2g**	130
2	4-$MeOC_6H_4NH_2$	5.29[14a,15b]	**2b**	114
3	$C_6H_5NH_2$	4.58[14a,15b]	**2a**	101
4	1-$C_{10}H_7$	4.11[15c]	**2e**	83
5	1-$C_{14}H_9NH_2$	3.85[15a]	**2f**	58
6	2,6-$Me_2C_6H_3NH_2$	3.89[15b]	**2c**	52
7	2,6-$iPr_2C_6H_3NH_2$	4.41[14a]	**2d**	0

In fact, on analyzing the pK_a value of anilines (Table 3),[14b,15] it appears that when the basicity of the anilines, and accordingly the coordination ability of the ligands is decreased,[14] the productivity of the corresponding catalysts diminishes (Table 3), possibly due to a higher decomposition rate. Thus, the productivity seems to be governed mainly by the catalyst stability, which correlates with the binding strength of the ligand.

Therefore, catalyst **2g** is the most active probably because of the high basicity of the anthryl ligand, which tends to stabilize the complex, dramatically reducing the deactivation rate. However, a stabilizing effect deriving from a π stacking interaction between the three condensed aromatic rings of **2g** and the styrene in the olefin insertion transition state cannot be ruled out (vide infra). Conversely, the steric hindrance at the ortho position, together with a lower basicity, causes a decrease of the productivity of the process involving **2e**,**f**,**c** (see Table 2, entries 7, 9 and 3). The steric effect is remarkable especially in the reaction with complex **2d**, which, despite a basicity almost comparable to that of **2a** for the corresponding anilines (4.41 vs 4.58), is not productive. In this case probably the isopropyl groups block the copolymerization due to a difficult access of monomers to the catalytic center (Table 2, entry 6).[14]

Concerning the effect of the solvent on the productivity, while in dichloromethane catalysts **2a−g** show a different performance, depending on the electronic and steric features, in TFE catalysts **2e−g**, with fused aromatic rings, have similar rather high activities, reaching a plateau of productivity at about 500 (g of CP) (g of Pd)$^{-1}$ (Table 4). We attribute this behavior to a stabilizing effect of the TFE solvent that prolongs the life of the catalysts **2e−g** in the reaction medium. This extra stabilization was previously ascribed to the higher acidity of the fluorinated alcohol;[16] however, a coordination of the CF_3 moiety of the alcohol to the metal center might play a role in the stabilization process of the catalyst, as highlighted by the X-ray structures of **4g**,**c** (vide infra). Regarding the effect of the monomer, a greater productivity of styrene in comparison to that of *p*-methylstyrene either in CH_2Cl_2 (130 and 142 (g of CP) (g of Pd)$^{-1}$; Table 2, entry 10, vs Table 4, entry 1) and in TFE (290 and 495 (g of CP) (g of Pd)$^{-1}$; Table 2, entry 11, vs Table 4, entry 2) was found, similarly to what was observed with palladium catalysts bearing meta-substituted aryl-BIAN ligands.[2f] This might be linked to an easier complexation of styrene versus *p*-methylstyrene due to a higher π^* acidity of the former compound.

In general, moderate to good results in terms of M_w (weight-average molecular weight) and polydispersity were achieved; M_w ranges from 4400 with catalyst **2e** (Table 2, entry 7) to 35000 for catalyst **2f** in TFE (Table 4, entry 4). We can identify different responses of M_w with the variation of the reaction conditions: for example, with TFE as the reaction medium an increase of M_w was detected (Table 2, compare entries 3 and 4), meanwhile the presence of benzoquinone gives a decrease of M_w and an increase of polydispersity (Table 2, entry 4 vs entry 5).[16a,e] Although an increase of CO pressure has a beneficial effect on the M_w of the polymer, we could record a detrimental effect regarding the polydispersity (Table 2, compare entries 12 and 10).

2.3. Copolymer Stereochemistry. The polyketones were characterized by means of ^{1}H NMR ($CDCl_3$) and ^{13}C NMR spectroscopy (1,1,1,3,3,3-hexafluoro-2-propanol/$CDCl_3$ 1/1 (v/v), 298 K), and their tacticity was evaluated by integrating the ^{13}C NMR resonances corresponding to the ipso carbon atoms of the aryl groups. The microstructures of copolymers range from atactic to isotactic even if achiral C_{2v} or C_s nitrogen ligands generally produce syndiotactic polyketones. Catalysts **2a** (Ar = Ph) and **2b** (Ar = 4-MeOPh) afforded regioregular *p*-methylstyrene/CO polyketones with an atactic microstructure[2a−c] (Table 2, entries 1 and 2), while a slight prevalence of the *ll* triad is observed for the copolymers produced by the hemihindered complexes **2e** (Ar = 1-$C_{10}H_7$) and **2f** (Ar = 1-$C_{14}H_9$) (53% and 45% *ll*, Table 2, entries 7 and 9). A remarkable increment of the isotactic component was instead observed using complexes **2c** (Ar = 2,6-MePh)[2a,c,d] and **2g** (Ar = 9-$C_{14}H_9$), which produced a copolymer with a value for the *ll* triad of 71% (Table 2, entries 3 and 10), in line with the highest value found in previous work.[2c] Similarly, with styrene as comonomer, prevailingly isotactic copolymer was obtained with **2e** (43% *ll*, Table 4, entry 3) and **2f** (46% *ll*, Table 4, entry 3), while **2g** (Ar = 9-$C_{14}H_9$) gave an isotactic polyketone with an *ll* value of 73% (Table 4, entry 2). As a result, stereoregularity is mainly dictated by the catalyst regardless of the nature of comonomer, solvent, and reaction conditions. As triad distribution points out[17] (*ll* = 73%, *ul*/*lu* = 25%, *uu* = 2%)

Table 4. CO/Styrene Copolymerization Results[a]

					triad (%)[c]				
entry	cat.	yield (g)[b]	CP (%)	productivity ((g of CP) (g of Pd)$^{-1}$)	*ll*	*ul*/*lu*	*uu*	n_l	$10^{-3}M_w$ (PDI)[d]
1[e]	**2g**	0.530	>99	142	71	26	3	7.2	25.7 (1.2)
2	**2g**	1.846	>99	495	73	25	2	6.8	10.0 (1.5)
3	**2e**	2.100	>99	564	43	47	10	2.8	12.0 (2.0)
4	**2f**	1.757	>99	472	46	46	8	3.0	35.9 (1.4)

[a]Reaction conditions: n_{Pd} = 0.035 mmol; volume of styrene 2.6 mL (21 mmol, Pd/olefin = 1/600); solvent 2,2,2-trifluoroethanol (2.8 mL); Pd/1,4-benzoquinone = 1/5; T = 26 °C; P_{CO} = 1 atm; t = 27 h. [b]Total yield of homopolymer (HP) and copolymer (CP). [c]Evaluated from the intensities of the ^{13}C NMR ipso carbon atom resonances. [d]PDI = M_w/M_n. [e]Solvent CH_2Cl_2, without 1,4-benzoquinone.

dx.doi.org/10.1021/om400887x | *Organometallics* XXXX, XXX, XXX−XXX

(Table 4 entry 2) and due to the achiral nature of the catalyst, junctions of the type ...*RRRSSS*... (...*SSSRRR*...) must be present along the polymer chains. As previously reported for **2c**, a ligand-assisted chain-end control mechanism should be responsible for the production of isotactic copolymer with **2g**.[8] Using the relationship $n_l = 1 + 2(ll)/(lu)$,[18] which takes into account the intensities of the isotactic (*ll*) and heterotactic (*ul*) triads, it was possible to calculate the average length of the isotactic sequences n_l, assuming a Bernoulli propagation model, commonly observed for copolymers obtained with these kinds of Pd-complexes. The stereoblock length with catalysts **2c**,**g** was around 7 (n_l), while with the hemihindered complexes this value was about 3.5 (Tables 2 and 4). The strong steric interactions between the methyl groups of the DAB backbone and the groups in the phenyl ortho positions constrain the phenyl rings to arrange almost perpendicularly with respect to the palladium mean coordination plane (vide infra).[8] This catalyst geometry, together with the conformation of the growing polymer chain, is able to select the same olefin enantioface within each stereoblock, producing isotactic copolymer. Since catalyst **2g** gives, in term of stereoregularity, results similar to those for **2c**, we attribute this behavior to an analogous disposition of the *N*-aryl rings. In this regard, the two model complexes **5g′**,**c′**,[19] intermediates of the copolymerization process,[2d,8] appear similarly hindered in the region close to the metal reaction center, as shown by their van der Waals surfaces, depicted in Figure 1.

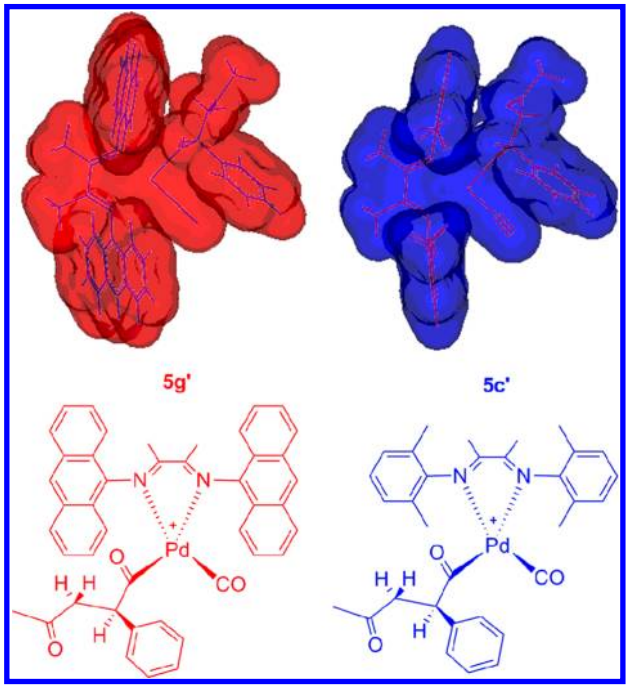

Figure 1. van der Waals surfaces of the carbonylated species **5g′** (left, red) and **5c′** (right, blue).

Finally, the next intermediate, having a structure similar to that of **5g′** but with the styrene in place of CO,[2d,8] was analyzed by rigid potential energy surface scans performed along both the N−Ar bonds (for details, see Computational Methods in the Experimental Section). A comparative analysis, performed for all analogous complexes with ligands **a**, **c**, **f** ,and **g**, shows that the 9-anthryl derivative is by far the most rigid.

In conclusion, introducing a new set of achiral diaryl diazabutadiene ligands with extended fused aromatic rings, we have optimized the copolymerization reaction under different conditions, achieving good results in terms of copolymer productivity, stereoregularity, and M_w. In particular, in chlorinated solvent we obtained good productivity, up to 130 (g of CP) (g of Pd)$^{-1}$ of stereoblock isotactic CO/*p*-methylstyrene polyketone, with a tacticity of 71%, M_w = 16700, and good polydispersity (1.2); meanwhile, by using fluorinated ethanol we attained excellent productivity, up to 500 (g of CP) (g of Pd)$^{-1}$ of CO/styrene copolymer with a tacticity of 73% (n_l = 7), M_w = 10000, and good polydispersity (1.5).

2.4. Mechanistic Studies: Synthesis and Characterization of Complexes 3g−6g. Initial steps of the copolymerization reaction were investigated to understand how the steric arrangement of the catalyst, bearing the achiral α-diimine **g**, is able to determine the stereoselective insertion of the olefin (Scheme 4). For this purpose, complex **3g** was used,

Scheme 4. First Intermediates of Copolymerization Reaction[a]

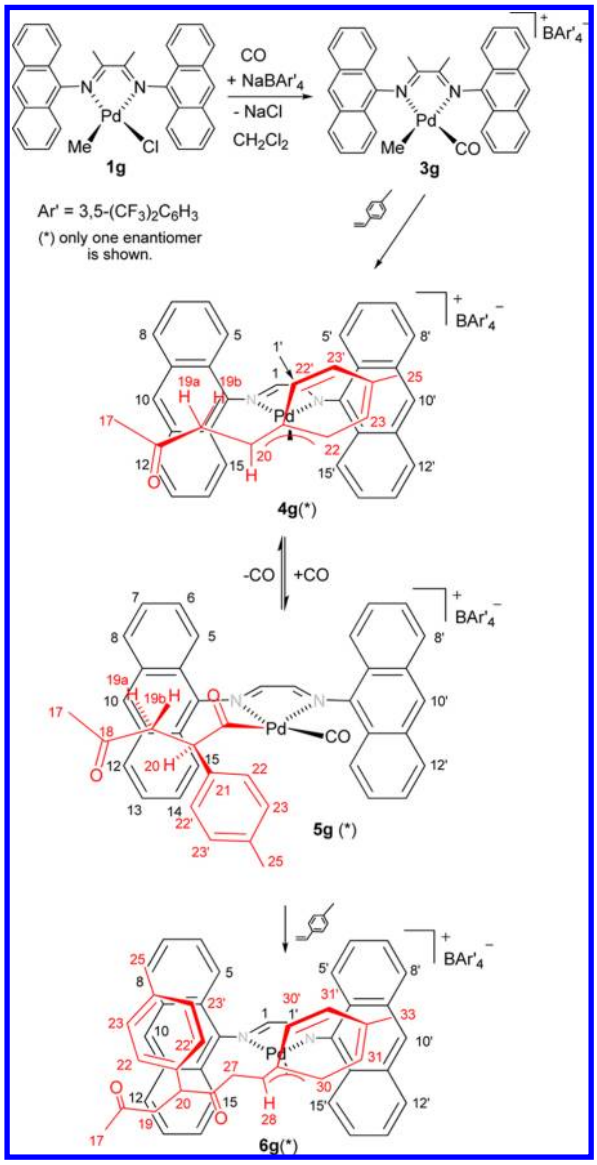

[a]For clarity 1,1′-methyls are not depicted in complexes **4g−6g**.

since it was previously observed that methyl acetonitrile Pd complexes with α-diimine ligands led, under a CO atmosphere,

dx.doi.org/10.1021/om400887x | *Organometallics* XXXX, XXX, XXX−XXX

to the corresponding methyl carbonyl derivatives that are the real catalytic initiators (Scheme 4).[20] In addition, the less coordinating tetraarylborate counterion was chosen to favor alkene insertion in the stoichiometric reactions.

The insertion of *p*-methylstyrene in the Pd−acetyl bond, derived from the methyl migration in **3g**, leads to complex **4g**, having the *p*-methylstyrene unit coordinated in an η^3-allyl fashion. Complex **4g** shows chemical shift values typical of allyl systems (C22−C22′, 107.2 ppm; C20, 54.8 ppm; H20, 2.73 ppm ($CDCl_3$, 4 °C)) and a considerable shielding of the H19a and H19b resonances (0.29 and 1.58 ppm, respectively) due to the anisotropy effects of the aryl rings of the nitrogen ligand. The NMR characterization in $CDCl_3$ allowed the determination of the intramolecular structure of **4g** (Scheme 4). The assignment of the ^{1}H resonances of the allyl fragment of **4g** was made on the basis of the dipolar and scalar interactions detected in the ^{1}H-NOESY and ^{1}H-COSY spectra, respectively, and confirmed with previous reported studies[2d] (see section 4.5.2 in the Experimental Section).

A comparative analysis between the ^{1}H NMR spectra of **4g** and **4c** was made. Interestingly the upfield shift of several ^{1}H resonances of the allyl fragment in **4g** was more pronounced than that observed for the analogous α-diimine complex $[Pd(\eta^3\text{-}C_{11}H_{13}O)((2,6\text{-}MePh)_2DABMe_2)]^+[BAr'_4]^-$ (**4c**) bearing the 2,6-dimethyl-substituted phenyl ring[2d] (Table 5).

Table 5. Chemical Shifts (^{1}H NMR, δ ppm) of the Growing Chain in the Intermediate Complexes 4g,c[2d] and 5g,c[2d]

	complex 4g[a]	complex 4c[a]	Δδ	complex 5g[b]	complex 5c[c]	Δδ
H25	0.92	1.79	0.87	2.06	2.22	0.16
H23/H23′	5.80	6.54	0.74	6.91	7.14	0.23
H22/H22′	6.11	6.33	0.22	6.77	7.01	0.24
H20	2.8	3.17	0.37	3.92	4.20	0.28
H19a	0.30	1.12	0.82	0.62	1.67	1.05
H19b	1.63	2.31	0.68	2.23	2.72	0.49
H17	1.33	1.89	0.56	1.61	1.92	0.31

[a]Conditions: $CDCl_3$, 4 °C. [b]Conditions: CD_2Cl_2, −17 °C. [c]Conditions: $CDCl_3$, 20 °C.

This could be reasonably ascribed to the larger size of the magnetic anisotropy shielding cone on top of the anthryl moiety in **4g** in comparison to the phenyl ring in **4c**. As a consequence, for example, the H23/H23′ resonances are observed at 6.54 ppm in **4c** and at 5.80 ppm in **4g**, and protons H22/H22′ are found at 6.33 ppm in **4c** and 6.11 ppm in **4g**. As expected, the value Δδ decreases on going from H25 to H23/H23′ and then to H22/H22′ (Scheme 4): i.e., from the external side of the nitrogen ligand toward the palladium center, moving away from the shielding cone of the anthracene ring. The same occurs on going from H19a, H19b to H20. These ^{1}H NMR upfield shifts of **4g** relative to the signals for **4c** could point toward a greater π stacking interaction in the former between the η^3-allylc moiety and the N-aryl counterpart.[21] A π stacking interaction, between the rings of the ligand and the styrene unit, could be present also in the olefin insertion transition states relative to intermediates **4g** and **6g**, producing the stabilization needed for the productivity of **2g** being greater than that of **2c**.

The next step of the copolymerization process was investigated by bubbling carbon monoxide into a CD_2Cl_2 solution of **4g** for 10 min at −70 °C. The NMR analysis reveals the formation of an equilibrium mixture between the starting species **4g** and the corresponding carbonylated product **5g** (Scheme 4). The equilibrium ratio appears to be affected by the temperature, and the maximum conversion in **5g** (60%) was observed at −17 °C after 3 days under an atmospheric pressure of CO. From the NMR analysis of **5g** (for details, see section 4.5.3 in the Experimental Section) some similarities with **4g** can be recognized. ^{1}H signals of protons H19a, H19b and H20 (0.62, 2.23, and 3.92 ppm, respectively) appear strongly shielded in comparison with those of the analogous complex bearing the $(i\text{Pr})_2DABMe_2$ ligand (2.67, 3.50, and 4.54 ppm, respectively).[20a] This suggests that they are located in the shielding cone of the aromatic rings of the N-anthryl ligand. Furthermore, since the ^{13}C resonance of C18 in **5g** (202.7 ppm) is notably different from the typical value reported for a palladium O-coordinated acetyl moiety (around 230 ppm),[10b,20,22] a six-membered chelate structure (with the acetyl linked to palladium[23]) was ruled out. In addition, both the NOE interactions involving the growing chain and the nitrogen ligand and the strong shielding effect observed for H19a, H19b and H20 give evidence in favor of the open-chain structure of complex **5g** (Scheme 4). The structure of **5g** in solution, depicted according to the NMR evidence, is in agreement with the fully optimized **5g′**[19] model (Figure 1) with the DFT method (see Computational Methods in the Experimental Section). Finally, the upfield shift of the ^{1}H resonances of the acetyl fragment in **5g** is more pronounced than that observed for the analogous α-diimine complex $[Pd\{C(O)CH(p\text{-}Me\text{-}C_6H_4)CH_2C(O)Me\}((2,6\text{-}Me_2Ph)_2DABMe_2)]^+[BAr'_4]^-$ (**5c**) bearing the 2,6-dimethyl-substituted phenyl ring[2d] (Table 5).

The addition of *p*-methylstyrene to the equilibrium mixture of **4g** and **5g** (40/60) in CD_2Cl_2 under 1 atm of carbon monoxide leads to the formation of the allyl intermediate **6g** as the major product (NMR yield 74%) (Scheme 4). NMR investigation reveals that **6g** exists prevalently as a single diastereoisomeric form that should correspond to a *RR* (or *SS*) configuration, considering the isotacticity of the copolymer obtained with the precatalyst **2g** (Scheme 1). Similarly to **4g**, in **6g** the growing chain is coordinated in an η^3-allyl fashion involving one double bond of the aryl ring of the second inserted olefin (Scheme 4). For analogous complexes bearing the $(2,6\text{-}Me_2Ph)_2DABMe_2$ ligand **c**, a 25/75 mixture of the two η^3-allyl complexes **4c** and **6c** was obtained instead.[2d] This different behavior outlines that the reaction performed with catalyst **2g** is much more efficient than that performed with **2c** and the process is efficiently driven toward the insertion of the new styrene unit. The analysis of the ^{1}H-NOESY spectrum of **6g** (see section 4.5.4 in the Experimental Section) depicts the molecular structure illustrated in Scheme 4; moreover, due to the presence of an aromatic ring in the growing chain H10, H8, and H12 resonances were quite shielded in **6g** (Table S3 in the Supporting Information).

As a result of the magnetic anisotropy shielding cone in **6g**, we suppose the presence of π stacking interactions that stabilize the **6g**-like intermediates, increasing their population.[21] In addition, a π stacking interaction could be responsible for lowering the energy transition of the olefin insertion reaction, driving the copolymerization process toward higher productivity.[21]

2.5. Solid-State Molecular Structures of Complexes 2g and 4g. The solid-state structure was obtained, by means of X-ray single-crystal studies, for catalyst **2g** and remarkably for intermediate **4g**, which proved to be stable enough to obtain crystals. The molecular structure of the catalyst **2g** is shown in

dx.doi.org/10.1021/om400887x | *Organometallics* XXXX, XXX, XXX−XXX

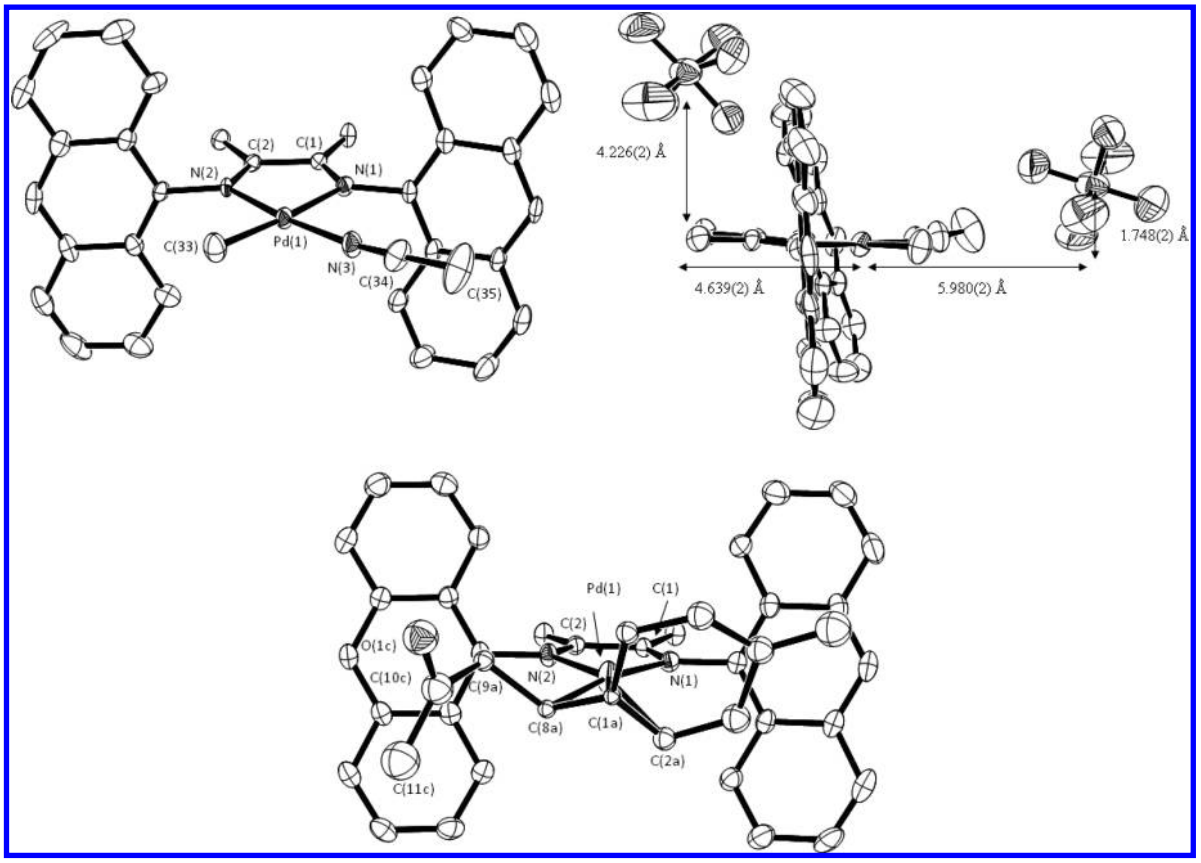

Figure 2. ORTEP 3 views of the complex cation of **2g** (top left), the relative cation−anion positions in **2g** (top right), and the complex cation of **4g** (bottom center). Hydrogen atoms have been omitted for sake of clarity. All atoms are drawn at 30% probability.

Figure 2 (selected bond lengths and angles are given in Table S2 in the Supporting Information).

The metal center adopts the usual square-planar coordination. Bond lengths and angles featuring the metal environment are in line with those of structural related complexes retrieved in the Cambridge Structural Database (CSD version 5.34, November 2012).[24]

Because of their size and due to the presence of the methyl groups on the back, both anthracene units are almost perpendicular with respect to the metal coordination mean plane (dihedral angles of 75.7(1) and 86.5(1)°). As a consequence of this arrangement, the four anthryl hydrogen atoms in 1- and 8- positions are facing each other, thus preventing the counterion from locating near the metal center. In fact, the closest counterion,[25] as already found in the crystal lattice of similar catalysts,[2c,26] is located in the back, above the diimine carbons of the nitrogen ligand (Figure 2), and weakly interacts with the aromatic hydrogen atoms of the ligand. Interestingly the interionic structure of **2g** closely resembles that found in a similar dimethyl ortho-substituted aryl α-diimine complex.[2c] The horizontal distance between the Pd atom and the intercept of the vertical distance which separates the P atom from the metal coordination mean plane[27] are roughly the same: 4.639(2) vs 4.723 Å (compare **2g** with **7a** in ref 2c), while in **2g** the PF_6^- ion is slightly higher with respect to the metal coordination mean plane (4.226(2) vs 3.994 Å). Finally, the next closest PF_6^- ion (related by the symmetry operation $-x + 1, y - {}^1/_2, -z + {}^1/_2$) is also shown in Figure 2, together with selected distances involving the phosphorus atoms in order to determine the position of both the anions with respect to the metal complex.[27]

The similarity between the interionic structures discussed above (**2g** vs **7a** in ref 2c) suggests that the anthracene units and the *o*-dimethylphenyl moieties cause comparable steric hindrance in the metal apical positions. As a consequence, for **2g**,**c** a similar accessibility of the carbonyl moiety and then of the monomers to the metal apical position should be expected. Thus, the steric features of **2g** must be balanced by the already mentioned high basicity of the corresponding diimine ligand and/or by a possible π stacking interaction between the aromatic ring of the growing chain and the anthracene ligand;[21] both effects could significantly trigger and enhance the productivity.

In the complex cation of intermediate **4g**, the palladium ion is coordinated to the *p*-methylstyrene unit in a η^3-allyl fashion, involving the C(1a) (C(1b)), C(2a) (C(2b)), and C(8a) (C(8b)) atoms (Figure 2). For the *p*-methylstyrene unit, which appears disordered except for the acetyl group, the two models **a** and **b** were found. The least-squares planes defined by the atoms of **a** and **b** are nearly coplanar. The three Pd−C bond distances are significantly different in model **a**, while in **b** they are comparable (Table S2 in the Supporting Information). The resulting coordination geometry about the metal ion can be conveniently described as distorted square planar (Table S2).

The four donor atoms (N(1), N(2), C(2a) (C(2b)) and C(8a) (C(8b))) define a mean plane which is almost perpendicular both to the anthracene units (about 65 and 75° for models **a** and **b**, respectively) and to the *p*-methylstyrene unit (79.4(2) and 76.8(2)° for **a** and **b**, respectively) (Figure 2). A comparison with structurally related complexes deposited in the CSD does not reveal any peculiar geometrical feature for

dx.doi.org/10.1021/om400887x | *Organometallics* XXXX, XXX, XXX−XXX

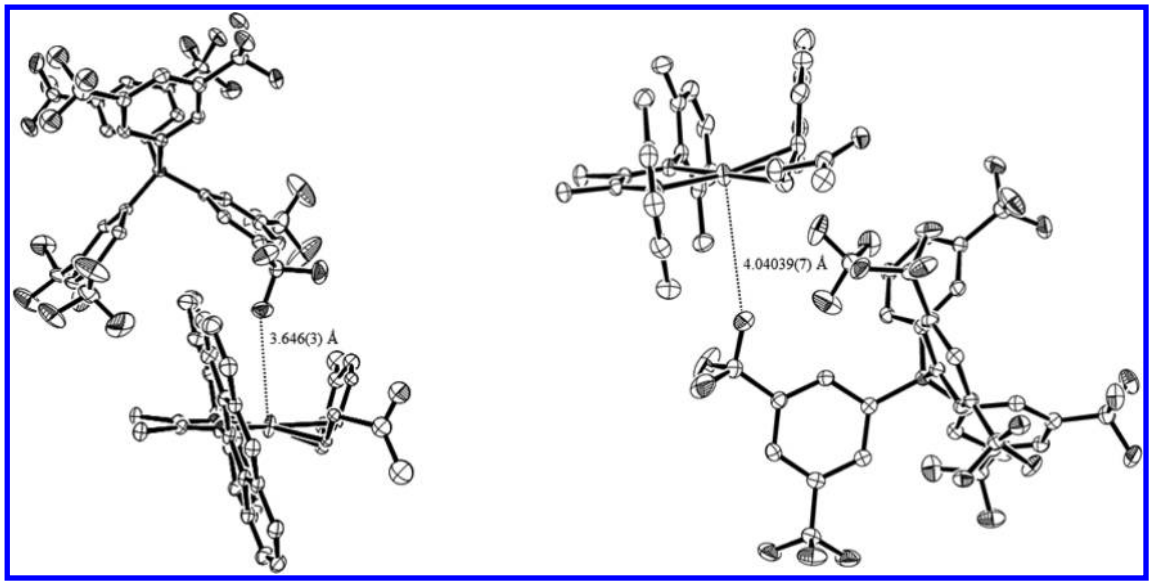

Figure 3. (left) Shape match between the cation and anion in the crystal lattice of **4g**. (right) Closest cation−anion interaction in the crystal lattice of **4c**.

the palladium complex. As shown in Figure 3, a good shape match between the two ions occurs in the crystal lattice: the closest BArF anion places a fluorine atom in the metal apical position 3.646(3) Å from the palladium cation. A longer Pd−F distance (ca. 4.0 Å) was found in the crystal structure of the analogous complex having the *o*-dimethyl substituted ligand **4c** (Figure 3, right).[2d] The unexpectedly short Pd−F distance in **4g** could indicate the presence of an interaction between the palladium and the fluoro atom that stabilizes the crystal lattice (Figure 3). A similar contact might occur between palladium complexes and the fluorinated alcohol in the copolymerization reaction carried out in TFE. In particular, we suppose that a Pd−F interaction might contribute to the catalyst stability, in combination with the acidity of the alcohol,[16] increasing the productivity in polyketones.[16]

To validate this hypothesis, a copolymerization reaction with catalyst **2g** was performed using α,α,α-trifluorotoluene as solvent, giving a copolymer yield of 423 (g of CP) (g of Pd)$^{-1}$, M_w = 24000 and a value for the *ll* triad of 75%; these data are comparable to those achieved carrying out the reaction in TFE (Table 4, entry 2).

3. CONCLUSION

In this paper we have shown the synthesis and coordination chemistry of a series of cationic Pd(II) complexes, bearing new α-diimine ligands with fused aromatic rings, and their application in CO/vinyl arene copolymerization. Among all species, the catalyst with the C_{2v}-symmetric 9-anthracenyl diimine ligand (9-$C_{14}H_9$)$_2$DABMe$_2$ (**g**) provides stereoblock isotactic CO/*p*-methylstyrene and CO/styrene polyketones in yields that are the highest reported for the stereoselective copolymerization of aromatic olefins with carbon monoxide using achiral nitrogen ligands. The structural analysis of the first steps of the CO/*p*-methylstyrene copolymerization revealed the stereoselective formation of the olefin/CO/olefin insertion product (**6g**), which prevalently exists in solution in only one diastereoisomeric form, thus justifying the observed high polymer isotacticity provided by complex **2g**. Moreover, both analyzing the copolymerization results and the structure of the first intermediates, we postulated that the donor capacity of the ligand, a possible π stacking interaction in the olefin insertion transition states, and fluoro−palladium interactions between catalyst and fluorinated alcohol, in combination with the alcohol acidity, could reasonably be the origin for the high productivity found with the new 9-anthryl catalyst.

4. EXPERIMENTAL SECTION

4.1. Materials and Methods. All manipulations were carried out under a nitrogen atmosphere by using Schlenk techniques. Solvents were dried by standard methods and freshly distilled under nitrogen. *p*-Methylstyrene (Aldrich) was dried over calcium hydride and distilled before use. Carbon monoxide (Cp grade 99.99%) was supplied by Air Liquide. CP grade chemicals were used as received unless otherwise stated. Chloroform-*d* and methylene chloride-d_2 were degassed and stored over 4 Å molecular sieves. Ligands **a**−**d**[28] and complexes **1a**−**c**,[1,2d,29] **1d**,[30] and **2b**,**c**[2d] were synthesized according to literature methods. NaBAr′$_4$ (Ar′ = 3,5-(CF$_3$)$_2$C$_6$H$_3$) was synthesized as previously reported.[31] Elemental analyses (C, H, N) were carried out with a Fisons Instruments 1108 CHNS-O Elemental Analyzer. Infrared spectra were measured in the range 4000−600 cm^{-1} on a Nicolet FT-IR Avatar 360 spectrometer. NMR spectra were measured on a Bruker Advance 200 spectrometer with a multinuclear 5 mm probe head. ^{1}H and ^{13}C NMR chemical shifts are relative to TMS and were measured using the residual proton or carbon resonance of the deuterated solvents.

4.2. Synthesis of Ligands e−g. *4.2.1. Synthesis of (N,N′E,N,N′E)-N,N′-(Butane-2,3-diylidene)dinaphthalen-1-amine (e).*

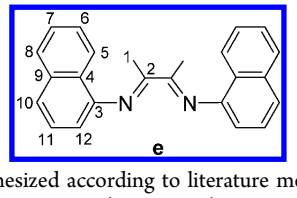

Ligand **e** was synthesized according to literature methods.[12] ^{1}H NMR (200.13 MHz, CDCl$_3$, 19 °C): δ 7.86 (m, 4H; H8 and H5), 7.68 (d, $^3J_{H,H}$ = 8.28 Hz, 2H; H10), 7.52 (m, 6H; H6, H7 and H11), 6.87 (d, 2H; H12), 2.33 ppm (s, 6H; H1). ^{13}C NMR (50.32 MHz, CDCl$_3$, 19 °C): δ 169.1 (s; C2), 147.0 (s; C3), 134.1 (s; C9), 128.1 (s; C8), 126.3 (s; C7), 125.8 (s; C11), 125.7 (s; C6), 125.5 (s; C4), 124.1 (s; C10), 123.4 (s; C5), 113.0 (s, C12), 16.0 ppm (s; C1). Anal. Calcd for C$_{24}$H$_{20}$N$_2$ (336.43): C, 85.68; H, 5.99; N, 8.33. Found: C, 85.73; H, 5.92; N, 8.37.

dx.doi.org/10.1021/om400887x | *Organometallics* XXXX, XXX, XXX−XXX

*4.2.2. Synthesis of (N,N′E,N,N′E)-N,N′-(Butane-2,3-diylidene)-dianthracen-1-amine (**f**).*

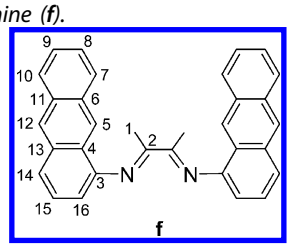

2,3-Butanedione (114 μL, 1.30 mmol) and 1 drop of formic acid were added to a solution of (1-$C_{14}H_9$)NH_2 (510 mg, 2.64 mmol) in methanol (6 mL), and the mixture was stirred for 48 h at 25 °C. The formed precipitate was collected by filtration, washed with methanol (2 × 10 mL), and dried under vacuum. The product was than solubilized in hot toluene (10 mL), precipitated with cold methanol, collected by filtration, washed with methanol (2 × 10 mL), and dried under vacuum. Ligand **f** was obtained as a brown powder (320 mg, 0.73 mmol; yield 56%). ^{1}H NMR (200.13 MHz, CD_2Cl_2, 19 °C): δ 8.53 (s, 2H; H12), 8.47 (s, 2H; H5), 8.08 (m, 4H; H10 and H7), 7.89 (d, $^3J_{H,H}$ = 7.2 Hz, 2H; H14), 7.55 (m, 6H; H15, H8 and H9), 6.89 (br d, 2H; H16), 2.45 ppm (s, 6H; H1). ^{13}C NMR (50.32 MHz, CD_2Cl_2, 19 °C): δ 169.4 (s; C2), 147.1 (s; C3), 132.3 (s; C6 or C11 or C13), 131.9 (s; C6 or C11 or C13), 131.4 (s; C6 or C11 or C13), 128.4 (s; C7 or C10), 128.0 (s; C7 or C10), 126.3 (s; C12), 125.7 (s; C8 or C9), 125.5 (s; C8 or C9), 125.3 (s; C15), 125.0 (s; C4), 124.3 (s; C14), 122.2 (s, C5), 111.4 (s; C16), 15.8 ppm (s; C1). Anal. Calcd for $C_{32}H_{24}N_2$ (436.55): C, 88.04; H, 5.54; N, 6.42. Found: C, 88.09; H, 5.50; N, 6.47.

*4.2.3. Synthesis of (N,N′E,N,N′E)-N,N′-(Butane-2,3-diylidene)-dianthracen-9-amine (**g**).*

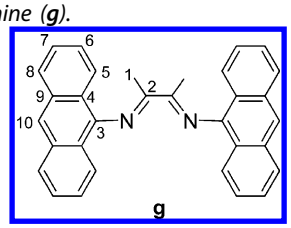

9-Aminoanthracene (9-$C_{14}H_9$)NH_2 was synthesized as follows: palladium on charcoal (10%, 30 mg) was added to a solution of 9-nitroanthracene (300 mg, 1.34 mmol) in ethyl acetate (15 mL). The reaction mixture was transferred into a steel autoclave which was charged with H_2 (3 atm) and stirred for 5.5 h at 20 °C. The mixture was then filtered under a nitrogen atmosphere, and the solvent was evaporated under vacuum. 9-Aminoanthracene was obtained as a yellow powder (242 mg, 1.25 mmol; yield 94%). ^{1}H NMR (200.13 MHz, $CDCl_3$, 19 °C): δ 7.98−7.90, 7.47−7.40 (m, 9H; aromatic protons), 4.87 ppm (br s, 2H; NH_2). Ligand **g** was synthesized as follows: 2,3-butanedione (85 μL, 0.97 mmol) and 1 drop of formic acid were added to a solution of (9-$C_{14}H_9$)NH_2 (374 mg, 1.94 mmol) in methanol (1 mL), and the mixture was stirred overnight at 25 °C. The formed precipitate was collected by filtration, washed with cold methanol, and dried under vacuum. Ligand **g** was obtained as an orange powder (245 mg, 0.56 mmol; yield 58%). ^{1}H NMR (200.13 MHz, CD_2Cl_2, 19 °C): δ 8.32 (s, 2H; H10), 8.10 (d, $^3J_{H,H}$ = 5.1 Hz, 4H; H8), 7.91 (d, $^3J_{H,H}$ = 4.3 Hz, 4H; H5), 7.56 (m, 8H; H6 and H7), 2.26 ppm (s, 6H; H1). ^{13}C NMR (50.32 MHz, CD_2Cl_2, 18 °C): δ 170.8 (s; C2), 143.1 (s; C3), 131.84 (s; C4), 128.4 (s; C8), 125.6 (s; C6 or C7), 125.2 (s; C7 or C6), 123.5 (s; C5), 121.8 (s; C10), 119.7 (s; C9), 16.9 ppm (s; C1). Anal. Calcd for $C_{32}H_{24}N_2$ (436.55): C, 88.04; H, 5.54; N, 6.42. Found: C, 88.00; H, 5.56; N, 6.45.

4.3. Synthesis of Complexes 1e−g. *4.3.1. General Procedure for the Synthesis of Complexes **1e−g**.* A solution of the appropriate ligand in 5 mL of dichloromethane was added to a solution of [Pd(Me)(Cl)(COD)] in 5 mL of the same solvent. The reaction mixture was stirred overnight at 25 °C. The solvent was reduced up to 2 mL by evaporation under vacuum, and diethyl ether (30 mL) was added to precipitate the desired compound. After filtration, the resulting solid was washed with diethyl ether (5 mL) and dried under vacuum.

*4.3.2. Synthesis of Pd(Me)Cl((1-$C_{10}H_7$)$_2$DABMe$_2$) (**1e**).*

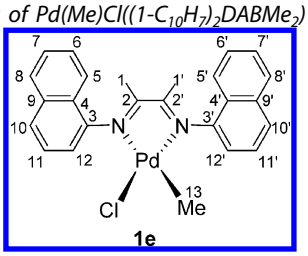

Reagents: (1-$C_{10}H_7$)$_2$DABMe$_2$ ligand, 200 mg (0.59 mmol); [Pd(Me)(Cl)(COD)], 158 mg (0.59 mmol). Yield: 148 mg (0.30 mmol, 50%) of **1e** as a red-orange powder. The NMR analysis indicated that the two possible conformational isomers, in which the nitrogen ligand adopts a C_2- or a C_s-symmetric coordination geometry, are simultaneously present in CD_2Cl_2 solution at 19 °C with an approximate equimolar ratio. ^{1}H NMR (200.13 MHz, $CDCl_3$, 19 °C): δ 7.96 (br d, 2H; H8(C_2 and C_s) and H8′(C_2 and C_s)), 7.93 (br d, 1H; H5′(C_2 and C_s)), 7.90 (br d, 1H; H5(C_2 and C_s)), 7.87 (br d, 1H; H10′) (C_2 and C_s), 7.82 (br d, 1H; H10(C_2 and C_s)), 7.59 (m, 6H; H6, (C_2 and C_s) H6′(C_2 and C_s), H7(C_2 and C_s), H7′(C_2 and C_s), H11(C_2 and C_s) and H11′(C_2 and C_s)), 7.18 (br dd, 1H; H12(C_2 and C_s)), 7.14 (br dd, 1H; H12′(C_2 and C_s)), 2.12 (s, 3H; H1(C_2 and C_s)), 2.06 (br s, 3H; H1′(C_2 and C_s)), 0.46 ppm (s, 3H; H13(C_2 and C_s)). ^{13}C NMR (50.32 MHz, $CDCl_3$, 19 °C) δ 175.7 (s; C2′(C_2 and C_s)), 170.3 (s; C2(C_2 and C_s)), 143.1, 143.0 (s; C3(C_2 and C_s)), 142.7 (s; C3′(C_2 and C_s)), 133.8 (s; C9(C_2 and C_s) and C9′(C_2 and C_s)), 128.66, 128.63, 128.56, 128.50 (s; C8(C_2 and C_s) and C8′(C_2 and C_s)), 127.5 (br s; C10′(C_2 and C_s) and C11(C_2 and C_s)), 127.2, 127.1, 126.8, 126.7 125.2 (s; C6(C_2 and C_s), C6′(C_2 and C_s), C7(C_2 and C_s), and C7′(C_2 and C_s)), 127.1 (s; C10(C_2 and C_s)), 126.5 (s; C11′(C_2 and C_s)), 125.5 (s; C4(C_2 and C_s) and C4′(C_2 and C_s))), 122.9, 122.8 (s; C5(C_2 and C_s)), 122.3, 122.2 (s; C5′(C_2 and C_s)), 117.6 (s; C12′(C_2 and C_s)), 117.1 (s, C12(C_2 and C_s)), 20.8 (s; C1′(C_2 and C_s)), 19.8 (s; C1(C_2 and C_s)), 2.8, 2.6 ppm (s; C13(C_2 and C_s)). Anal. Calcd for $C_{25}H_{23}ClN_2Pd$ (493.33): C, 60.86; H, 4.70; N, 5.68. Found: C, 60.80; H, 4.66; N, 5.63.

*4.3.3. Synthesis of Pd(Me)Cl((1-$C_{14}H_9$)$_2$DABMe$_2$) (**1f**).*

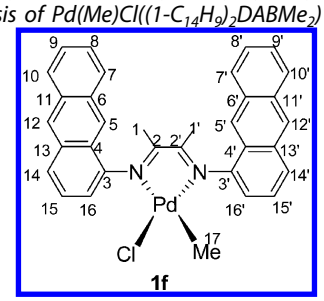

Reagents: (1-$C_{14}H_9$)$_2$DABMe$_2$ ligand, 100 mg (0.23 mmol); [Pd(Me)(Cl)(COD)], 56 mg (0.21 mmol). Yield: 83 mg (0.14 mmol, 67%) of **1f** as a brown powder. The NMR analysis indicated that the two possible conformational isomers, in which the nitrogen ligand adopts a C_2- or a C_s-symmetric coordination geometry, are simultaneously present in CD_2Cl_2 solution at 19 °C with an approximate equimolar ratio. ^{1}H NMR (200.13 MHz, CD_2Cl_2, 4 °C): δ 8.78−8.52 (m; 4H; H12(C_2 and C_s), H12′(C_2 and C_s), H5(C_2 and C_s), H5′(C_2 and C_s)), 8.32 (t, 1H; H7(C_2 and C_s)), 8.20 (brt, 1H; H7′(C_2 and C_s)), 8.08 (m, 4H; H10(C_2 and C_s), H10′(C_2 and C_s), H14(C_2 and C_s) and H14′(C_2 and C_s)), 7.63 (m, 6H; H8(C_2 and C_s), H8′(C_2 and C_s), H9(C_2 and C_s), H9′(C_2 and C_s), H15(C_2 and C_s) and H15′(C_2 and C_s)), 7.23 (m, 2H; H16(C_2 and C_s) and H16′(C_2 and C_s)), 2.23, 2.15 (s, 6H; H1(C_2 and C_s) and H1′(C_2 and C_s)), 0.28, 0.27 ppm (s, 3H; H17(C_2 and C_s)). ^{13}C NMR (50.32 MHz, CD_2Cl_2, 19 °C) δ 176.84 (s; C2′(C_2 and C_s) or C2(C_2 and C_s)), 171.59 (s; C2(C_2 and C_s) or C2′(C_2 and C_s)), 143.6 (br s; C3′(C_2 and C_s) and C3(C_2 and C_s)), 132.21, 132.09, 131.99, 131.67 (s; C11(C_2 and C_s), C11′(C_2 and C_s), C13(C_2 and C_s), C13′(C_2 and C_s), C6(C_2 and C_s), C6′(C_2 and C_s), C4(C_2 and C_s) and C4′(C_2 and C_s)), 128.43 (s; C7(C_2 and C_s)), 128.11 (br s; C7′(C_2 and C_s)), 127.42 (s; C12(C_2 and C_s) or C12′(C_2 and C_s)), 127.07 (br s; C12′(C_2

dx.doi.org/10.1021/om400887x | *Organometallics* XXXX, XXX, XXX−XXX

and C_s) or C12(C_2 and C_s)), 128.11, 127.7, 127.07 (br s; C10(C_2 and C_s), C10′(C_2 and C_s), C14(C_2 and C_s) and C14′(C_2 and C_s)), 126.36, 126.00 (br s; C9(C_2 and C_s), C9′(C_2 and C_s), C15(C_2 and C_s) and C15′(C_2 and C_s)), 124.31, 124.14 (s; C8(C_2 and C_s) and C8′(C_2 and C_s)), 121.71, 121.00 (C5(C_2 and C_s) and C5′(C_2 and C_s)), 117.06, 115.86 (s; C16(C_2 and C_s) and C16′(C_2 and C_s)), 20.83, 19.75 (s; C1(C_2 and C_s) and C1′(C_2 and C_s)), 1.23 ppm (s; C17(C_2 and C_s)). Anal. Calcd for $C_{33}H_{27}ClN_2Pd$ (593.45): C, 66.79; H, 4.59; N, 4.72. Found: C, 66.82; H, 4.60; N, 4.72.

*4.3.4. Synthesis of Pd(Me)Cl((9-$C_{14}H_9$)$_2$DABMe$_2$) (**1g**).*

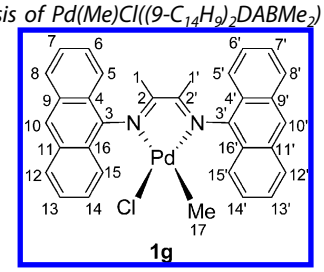

1g

Reagents: (9-$C_{14}H_9$)$_2$DABMe$_2$ ligand, 167 mg (0.38 mmol); [Pd(Me)(Cl)(COD)], 87 mg (0.32 mmol). Yield: 145 mg (0.24 mmol, 75%) of **1g** as a brown powder. ^{1}H NMR (200.13 MHz, CD_2Cl_2, 19 °C): δ 8.59 (s, 1H; H10 or H10′), 8.51 (s, 1H; H10′ or H10), 8.23–8.12 (m, 8H; H8, H8′, H12, H12′, H5, H5′, H15 and H15′), 7.81–7.60 (m, 8H; H7, H7′, H6, H6′, H13, H13′, H14 and H14′), 2.05 (s, 3H; H1), 1.98 (s, 3H; H1′), 0.05 ppm (s, 3H; H17); ^{13}C NMR (50.32 MHz, CD_2Cl_2, 19 °C) δ 177.6 (s; C2′), 172.8 (s; C2), 144.8 (s; C3 and C3′), 131.1 (s; C4, C4′, C16 and C16′), 129.0 (s; C8′ or C12′ or C8 or C12), 128.9 (s; C8′ or C12′ or C8 or C12), 128.8 (s; C8 or C12 or C8′ or C12′), 128.7 (s; C8 or C12 or C8′ or C12′), 127.5 (s; (C7 and C13) or (C7′ and C13′)), 126.6 (s; C10 or C10′), 126.4 (s; (C7′ and C13′) or (C7 and C13)), 126.1 (s; (C6 and C14) or (C6′ and C14′)), 125.8 (s; (C6′ and C14′) or (C6 and C14), 125.5 (s; C10′ or C10), 122.9 (s; (C5 and C15) or (C5′ and C15′)), 122.0 (s; (C5′ and C15′) or (C5 and C15)), 115.9 (s; C9 and C9′ and C11 and C11′), 20.8 (s, C1′), 19.9 (s; C1), 0.81 (s; C17). Anal. Calcd for $C_{33}H_{27}ClN_2Pd$ (593.45): C, 66.79; H, 4.59; N, 4.72. Found: C, 66.84; H, 4.63; N, 4.74.

4.4. Synthesis of Complexes 2a,d–g. *4.4.1. General Procedure for the Synthesis of Complexes **2a,d–2g**.* $AgPF_6$ was added to a dichloromethane/acetonitrile (5/1) solution (6 mL) of **1a,d–g** cooled at 0 °C. The mixture was allowed to react for 2 h, during which time AgCl precipitated. The mixture was filtered through Celite, and a solid was obtained after evaporation of the solvent under vacuum. The solid gave the desired complex on treatment with hexane (2 × 5 mL).

*4.4.2. Synthesis of [Pd(Me)(MeCN)(Ph$_2$DABMe$_2$)]$^+$[PF$_6$]$^-$ (**2a**).*

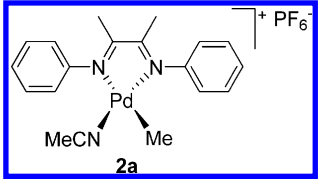

2a

Reagents: $AgPF_6$, 55 mg (0.22 mmol); **1a**, 80 mg (0.20 mmol). Yield: 65 mg (0.12 mmol, 60%) of **2a** as a yellow powder. ^{1}H NMR (200.13 MHz, $CDCl_3$, 19 °C): δ 7.47, 7.33, 7.13, 6.99 (10H; aromatic protons), 2.32, 2.26 (3H each; ligand backbone protons), 1.92 (s, 3H; Pd-NCCH_3), 0.41 (s, 3H; Pd-CH_3). ^{13}C NMR (50.32 MHz, $CDCl_3$, 19 °C) 180.7, 171.6, 132.9, 132.7, 130.6, 130.4, 128.8, 128.5, 122.1, 21.5, 19.7, 6.2, 3.0. Anal. Calcd for $C_{19}H_{22}F_6N_3PPd$ (543.78): C, 41.97; H, 4.08; N, 7.73. Found: C, 41.92; H, 4.03; N, 7.77.

*4.4.3. Synthesis of [Pd(Me)(MeCN)((2,6-i-Pr$_2$Ph)$_2$DABMe$_2$)]$^+$[PF$_6$]$^-$ (**2d**).*

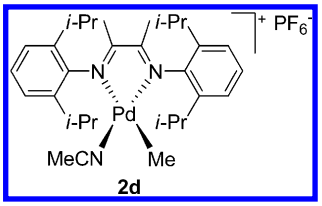

2d

Reagents: $AgPF_6$, 30.5 mg (0.11 mmol); **1d**, 70 mg (0.11 mmol). Yield: 61 mg (0.086 mmol, 78%) of **2d** as a yellow powder. ^{1}H NMR (200.13 MHz, CD_2Cl_2, 19 °C): δ 7.32 (m, 6H; aromatic protons), 2.99 (sept, 4H; $-CH(CH_3)_2$), 2.35 (s, 6H; ligand backbone protons), 1.83 (s, 3H; Pd-NCCH_3), 1.38 (d, $^2J_{HH}$ = 6.8 Hz, 3H; $-CH(CH_3)_2$), 1.33 (d, $^2J_{HH}$ = 6.8 Hz, 3H; $-CH(CH_3)_2$), 1.28 (d, $^2J_{HH}$ = 6.9 Hz, 3H; $-CH(CH_3)_2$), 1.24 (d, $^2J_{HH}$ = 6.9 Hz, 3H; $-CH(CH_3)_2$), 0.42 (s, 3H; Pd-CH_3). ^{13}C NMR (50.32 MHz, $CDCl_3$, 19 °C) 179.8, 174.6, 141.8, 141.2, 137.6, 137.2, 128.8, 128.2, 126.3, 125.6, 122,8, 30.5, 29.6, 24.2, 23.8, 23,5, 23.2, 21.8, 20.5, 7.2, 2.8. Anal. Calcd for $C_{31}H_{46}F_6N_3PPd$ (712.01): C, 52.29; H, 6.51; N, 5.90. Found: C, 52.22; H, 6.47; N, 5.86.

*4.4.4. Synthesis of [Pd(Me)(MeCN)((1-$C_{10}H_7$)$_2$DABMe$_2$)]$^+$[PF$_6$]$^-$ (**2e**).*

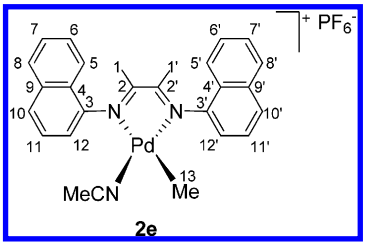

2e

Reagents: $AgPF_6$, 50 mg (0.2 mmol); **1e**, 90 mg (0.182 mmol). Yield: 114 mg (0.18 mmol, 98%) of **2e** as a yellow-orange crystalline powder. The NMR analysis indicated that the two possible conformational isomers, in which the nitrogen ligand adopts a C_2- or a C_s-symmetric coordination geometry, are simultaneously present in CD_2Cl_2 solution at 19 °C with an approximate equimolar ratio. ^{1}H NMR (200.13 MHz, $CDCl_3$, 19 °C): δ 8.25 (d, $^2J_{HH}$ = 8.2 Hz; H5(C_2) or H5(C_s)), 8.17 (d, $^2J_{HH}$ = 8.2 Hz; H5(C_s) or H5(C_2)), 7.96 (m, 3H; H5′(C_s and C_2), H8(C_s and C_2) and H8′(C_s and C_2)), 7.85 (d, 2H; H10(C_s and C_2) and H10′(C_s and C_2)), 7.66 (m, 6H; H6(C_s and C_2), H6′(C_s and C_2), H7(C_s and C_2), H7′(C_s and C_2), H11(C_s and C_2) and H11′(C_s and C_2)), 7.45 (d, $^2J_{HH}$ = 4.7 Hz; H12(C_s or C_2)), 7.41 (d, $^2J_{HH}$ = 4.7 Hz; H12(C_2 or C_s)), 7.37 (d, $^2J_{HH}$ = 7.5 Hz; H12′(C_s or C_2)), 7.30 (d, $^2J_{HH}$ = 7.5 Hz; H12′(C_2 or C_s)), 2.42 (s, 3H; H1(C_s and C_2)), 2.28, 2.29 (s, 3H; H1′(C_s and C_2)), 1.338, 1.331 (s, 3H; NCCH_3(C_s and C_2)), 0.18, 0.19 ppm (s, 3H; H13(C_s and C_2)). ^{13}C NMR (50.32 MHz, $CDCl_3$, 19 °C) δ 182.78, 182.68 (s; C2′(C_s and C_2)), 173.94, 173.81 (s; C2(C_s and C_2)), 142.02, 141.88, 141.83 (s; C3(C_s and C_2) and C3′(C_s and C_2)), 133.63, 133.57 (s; C9(C_s and C_2) and C9′(C_s and C_2)), 128.62, 128.30, 128.07, 127.76 (s; C8(C_s and C_2) and C8′(C_s and C_2)), 127.76, 127.19 (s; C10(C_s and C_2) and C10′(C_s and C_2)), 127.19 (br s; C7(C_s and C_2), C7′(C_s and C_2), C6(C_s and C_2) and C6′(C_s and C_2)), 125.94, 125.79, 125.48, 125.20, 125.20, 125.11 (s; C4(C_s and C_2), C4′(C_s and C_2), C11(C_s and C_2) and C11′(C_s and C_2)), 123.75, 123.39 (s; C5(C_s and C_2)), 122.54, 122.03 (s; C5′(C_s and C_2)), 120.82 (br s; CH_3CN(C_s and C_2)), 118.49, 118.17 (s; C12′(C_s and C_2)), 117.43, 117.23 (s; C12(C_s and C_2)), 21.08 (s; C1′(C_s and C_2)), 19.57 (s; C1(C_s and C_2)), 4.43, 4.37 (s; C13(C_s and C_2)), 1.33 ppm (br s; CH_3CN(C_s and C_2)). Anal. Calcd for $C_{27}H_{26}F_6N_3PPd$ (643.91): C, 50.36; H, 4.07; N, 6.53. Found: C, 50.40; H, 4.10; N, 6.55.

dx.doi.org/10.1021/om400887x | *Organometallics* XXXX, XXX, XXX–XXX

*4.4.5. Synthesis of [Pd(Me)(MeCN)((1-$C_{14}H_9$)$_2$DABMe$_2$)]$^+$[PF_6]$^-$ (**2f**).*

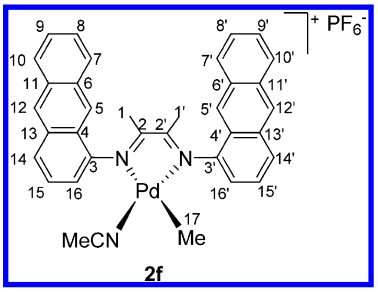

Reagents: $AgPF_6$, 33 mg (0.13 mmol); **1f**, 70 mg (0.118 mmol). Yield: 58 mg (0.078 mmol, 66%) of **2f** as a brown powder. The NMR analysis indicated that the two possible conformational isomers, in which the nitrogen ligand adopts a C_2- or a C_s-symmetric coordination geometry, are simultaneously present in CD_2Cl_2 solution at 19 °C with an approximate equimolar ratio. ^{1}H NMR (200.13 MHz, CD_2Cl_2, 19 °C): δ 8.78, 8.59, 8.53 (s, 2H; H5(C_2 and C_s) and H5′(C_2 and C_s)), 8.50 (m, 2H; H12(C_2 and C_s) and H12′(C_2 and C_s)), 8.38 (br d, 2H; H7(C_2 and C_s) and H7′(C_2 and C_s)), 7.99−7.92 (mbr, 4H; H10(C_2 and C_s), H10′(C_2 and C_s), H14(C_2 and C_s) and H14′(C_2 and C_s)), 7.65−7.21 (m, 8H; H8(C_2 and C_s), H8′(C_2 and C_s), H9(C_2 and C_s), H9′, H16(C_2 and C_s), H16′(C_2 and C_s), H15(C_2 and C_s) and H15′(C_2 and C_s)), 2.41, 2.40, 2.28 (s, 6H; H1(C_2 and C_s) and H1′(C_2 and C_s)), 1.02 (br s, 3H; NCCH_3(C_2 and C_s)), 0.12, 0.07 ppm (s, 3H; H17(C_2 and C_s)). ^{13}C NMR (50.32 MHz, $CDCl_3$, 19 °C) δ 183.06, 182.94 (s; C2(C_2 and C_s) or C2′(C_2 and C_s)), 174.17, 173.94 (s; C2′(C_2 and C_s) or C2(C_2 and C_s)), 142.16, 142.01, 141.8 (s; C3(C_2 and C_s) and C3′(C_2 and C_s)), 132.48−131.78 (br; C11(C_2 and C_s), C11′(C_2 and C_s), C13(C_2 and C_s), C13′(C_2 and C_s), C6(C_2 and C_s) and C6′(C_2 and C_s)), 130.93 (br s; C4(C_2 and C_s) and C4′(C_2 and C_s)), 129.30, 129.03 (s; C7(C_2 and C_s) and C7′(C_2 and C_s)), 128.22, 128.15, 128.04, 127.96, 127.72, 127.49, 127.29, 126.86, 126.70, 126.60, 126.43, 126.23 (s; C8(C_2 and C_s), C8′(C_2 and C_s), C10(C_2 and C_s), C10′(C_2 and C_s), C14(C_2 and C_s), C14′(C_2 and C_s), C12(C_2 and C_s), C12′(C_2 and C_s) and [(C15′(C_2 and C_s) and C15(C_2 and C_s)) or (C9′(C_2 and C_s) and C9(C_2 and C_s))], 124.95, 124.84, 124.36, 124.16 (s; (C9(C_2 and C_s) and C9′(C_2 and C_s)) or (C15(C_2 and C_s) and C15′(C_2 and C_s)), 122.78, 122.51, 121.41, 121.14 (s; C5(C_2 and C_s) and C5′(C_2 and C_s)), 120.19 (br s; CH_3CN(C_2 and C_s)), 117.82, 117.68, 116.36 (s; C16(C_2 and C_s) and C16′(C_2 and C_s)), 21.10, 19.59, 19.48 (s; C1(C_2 and C_s) and C1′(C_2 and C_s)), 4.53, 4.33 (s; C17(C_2 and C_s)), 1.17 ppm (br s; CH_3CN). Anal. Calcd for $C_{35}H_{30}F_6N_3PPd$ (744.00): C, 56.50; H, 4.06; N, 5.65. Found: C, 56.55; H, 4.08; N, 5.65.

*4.4.6. Synthesis of [Pd(Me)(MeCN)((9-$C_{14}H_9$)$_2$DABMe$_2$)]$^+$[PF_6]$^-$ (**2g**).*

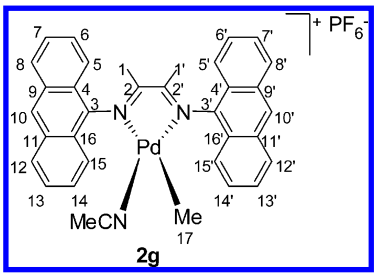

Reagents: $AgPF_6$, 37.4 mg (0.148 mmol); **1g**, 80 mg (0.135 mmol). Yield: 97 mg (0.13 mmol, 96%) of **2g** as a brown-violet powder. ^{1}H NMR (200.13 MHz, CD_2Cl_2, 4 °C): δ 8.64 (s, 1H; H10′), 8.62 (s, 1H; H10), 8.22 (br d, 6H; H8, H12, H8′, H12′,H5 and H15), 8.11 (br d, 2H; H5′ and H15′), 7.83 (m, 4H; H6, H14, H6′ and H14′), 7.71 (m, 4H; H7, H13, H7′ and H13′), 2.32 (s, 3H; H1), 2.23 (s, 3H; H1′), 1.16 (s, 3H; NCCH_3), 0.03 ppm (s, 3H; H17). ^{13}C NMR (50.32 MHz, CD_2Cl_2, 4 °C): δ 183.98 (s; C2′), 175.51 (s; C2), 136.19 (s; C3), 135.89 (s; C3′), 131.20 (s; (C4 and C16) or (C4′ and C16′)), 130.97 (s; (C4′ and C16′) or (C4 and C16)), 129.12 (s; (C8 and C12) or (C8′ and C12′)), 128.96 (s; (C8′ and C12′) or (C8 and C12)), 128.11 (s; (C6 and C14) or (C6′ and C14′)), 127.79 (s; (C6′ and C14′) or (C6 and C12)), 127.45 (s; C10′), 126.77 (s; C10), 126.36 (s; (C7 and C13) or (C7′ and C13′)), 126.30 (s; (C7′ and C13′) or (C7 and C13)), 122.56 (s; C5 and C15), 122.19 (s; (C9 and C11) or (C9′ and C11′)), 121.67 (s; C5′ and C15′), 121.56 (s; (C9′ and C11′) or (C9 and C11)), 120.98 (s; $NCCH_3$), 21.30 (s; C1′), 20.37 (s; C1), 4.15 (s; C17), 1.49 ppm (s; $NCCH_3$). Anal. Calcd for $C_{35}H_{30}F_6N_3PPd$ (744.00): C, 56.50; H, 4.06; N, 5.65. Found: C, 56.56; H, 4.10; N, 5.65.

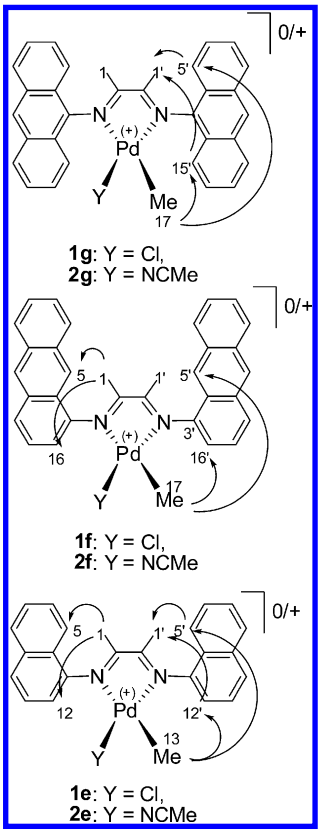

*Intramolecular Structures of Complexes **1e−g** and **2e−g**, Determined by NMR Experiments.* The Pd−Me resonance (H17, in **1e−g** and **2e−g**) was used as the starting point for the assignment of the protons of complexes **1g** and **2g**, because its chemical shift is known from previous studies and it is well separated from other resonances (H17 in **1g** is at 0.05 ppm (CD_2Cl_2, 19 °C) and in **2g** at −0.03 ppm ($CDCl_3$, 19 °C)).

Signals of the nitrogen ligand were essentially assigned on the basis of intramolecular dipolar interactions detected in the ^{1}H-NOESY spectrum. The H17 protons strongly interact with the aromatic H5′ and H15′ protons, which give interactions with CH_3(1′), allowing assignment of the ligand backbone resonances CH_3(1′) and CH_3(1). The other protons were then assigned from either the ^{1}H-COSY or ^{1}H-NOESY spectra, while their carbons were identified by ^{1}H,^{13}C-HSQC and ^{1}H,^{13}C-HMBC spectra. Also in the case of complexes **1e,f** and **2e,f** the Pd−Me resonance was helpful to assign aromatic protons. In compounds **1e** and **2e** H13 showed a strong NOE contact with H12′ and H5′. The interactions of the latter with CH_3(1′) allow discrimination between CH_3(1′) and CH_3(1). At the same time, CH_3(1) interacts both with H12 and H5 of the other half of the ligand. H5−H5′ and H12−H12′ are well separated in the ^{1}H NMR spectrum (for example, in **1e**: H5′, 7.93; H5, 7.90; H12, 7.18; H12′, 7.14 ppm ($CDCl_3$, 19 °C)). Similarly, in **1f** and **2f** NOE interactions of Pd−Me protons with H5′ and H16′ and those of CH_3(1) with H5 and H16 define the structures of complexes, and the remaining ^{1}H and ^{13}C resonances were then assigned following scalar and dipolar interactions.

dx.doi.org/10.1021/om400887x | *Organometallics* XXXX, XXX, XXX−XXX

4.5. Synthesis and Characterization of the First Intermediates 3g–6g in the CO/*p*-Methylstyrene Copolymerization Reaction.

*4.5.1. Synthesis of [Pd(Me)(CO)((9-$C_{14}H_9$)$_2$DABMe$_2$)]$^+$[BAr′$_4$]$^-$ (**3g**).*

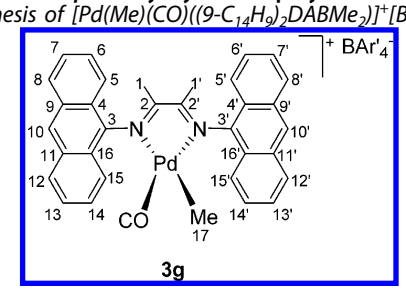

A 60 mg (0.101 mmol) sample of **1g** and a 93.4 mg (0.105 mmol) sample of NaBAr′$_4$ were dissolved at 0 °C in dichloromethane (4 mL) previously saturated with CO. The reaction mixture was filtered through Celite to remove NaCl. The solvent was evaporated under vacuum, and the resulting oil was washed with hexane (3 × 5 mL). A 119.5 mg (0.08 mmol, yield 81%) sample of **3g** was collected as a violet powder. ^{1}H NMR (200.13 MHz, $CDCl_3$, −20 °C): δ 8.67 (s, 1H; H10′), 8.65 (s, 1H, H10), 8.23 (m, 4H; H8, H8′, H12 and H12′), H87 (br d, 2H; H5 and H15), 7.71 (s, 10H; H5′, H15′ and Ar′-H_o), 7.64 (m, 8H; H7, H7′, H13, H13′, H6, H6′, H14 and H14′), 7.49 (s, 4H; Ar′-H_p), 2.30 (s, 3H; H1′), 2.27 (s, 3H; H1), 0.40 ppm (s, 3H; H17). ^{13}C NMR (50.32 MHz, $CDCl_3$, −20 °C): δ 186.5 (s; C2), 177.3 (s; C2′), 173.7 (s; CO), 161.5 (q, ^1J (C,B) = 49.5 Hz; Ar′-C_i), 136.7 (s; C3), 134.8 (s; Ar′-C_o), 132.7 (s; C3′), 131.1 (s; (C4 and C16) or (C4′ and C16′)), 130.9 (s; (C4′ and C16′) or (C4 and C16)), 130.1 (s; (C8 and C12) or (C8′ and C12′)), 129.9 (s; C8′ and C12′) or (C8 and C12)), 129.0 (s; (C6, C14, C6′ and C14′) or (C7, C13, C7′ and C13′) C10 and C10′), 128.6 (q, $^2J_{C,F}$ = 27.0 Hz; Ar′-C_m), 126.6 (s; (C7, C13, C7′ and C13′) or (C6, C14, C6′ and C14′)), 124.2 (q, $^1J_{C,F}$ = 267.7 Hz; CF_3), 121.9 (s; C9′ and C11′), 120.6 (s; C9, C11, C5 and C15), 120.1 (s; C5′ and C15′), 117.6 (s; Ar′-C_p), 21.9 (s; C1′), 20.6 (s; C1), 8.3 ppm (s; C17). Anal. Calcd for $C_{66}H_{39}F_{24}N_2OBPd$ (1449.22): C, 54.70; H, 2.71; N, 1.93. Found: C, 54.77; H, 2.80; N, 1.94.

*4.5.2. Synthesis of [Pd(η^3-$C_{11}H_{13}O$)((9-$C_{14}H_9$)$_2$DABMe$_2$)]$^+$[BAr′$_4$]$^-$ (**4g**).*

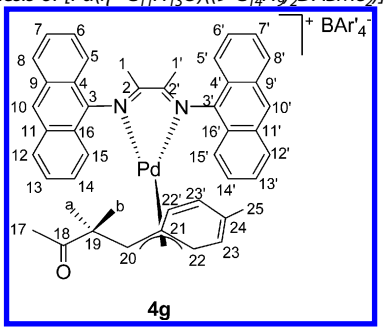

A 82.3 mg (0.056 mmol) sample of **3g** was dissolved in dichloromethane (5 mL) at 0 °C; then *p*-methylstyrene (7.5 μL, 0.056 mmol) was added. After 1 h the solution was filtered trough Celite and the solvent was evaporated under vacuum. The resulting oil was washed with hexane (2 × 3 mL) to yield complex **4g** (83 mg, 0.053 mmol, yield 95%) as a red-brown powder. ^{1}H NMR (200.13 MHz, $CDCl_3$, 4 °C): δ 8.70 (s, 1H; H10), 8.68 (s, 1H; H10′), 8.33 (br d, 1H; H15), 8.29 (br d, 2H; H8 and H12), 8.28 (br d, 1H; H12′), 8.19 (d, $^3J_{H,H}$ = 8.4 Hz, 1H; H8′), 8.07 (d, $^3J_{H,H}$ = 8.6 Hz, 1H; H15′), 7.89–7.58 (m, 18H; Ar′-H_o, Ar′-H_p, H6, H14, H14′, H7, H13, H13′), 7.70 (brt, 1H; H7′), 7.66 (br d, 1H; H5), 7.50 (brt, 1H; H6′), 7.18 (d, $^3J_{H,H}$ = 8.6 Hz, 1H; H5′), 6.11 (br d, 2H; H22 and H22′), 5.80 (d, 2H; H23 and H23′), 2.80 (dd, $^3J_{H,H}$ = 4.2 Hz and $^3J_{H,H}$ = 9.5 Hz, 1H; H20), 2.24 (s, 3H; H1′), 2.14 (s, 3H; H1), 1.63 (dd, $^3J_{H,H}$ = 9.4 Hz and $^2J_{H,H}$ = 18.5 Hz, 1H; H19b), 1.33 (s, 3H; H17), 0.92 (s, 3H; H25), 0.30 (dd, $^3J_{H,H}$ = 4.3 Hz and $^2J_{H,H}$ = 18.8 Hz, 1H; H19a). ^{13}C NMR (50.32 MHz, $CDCl_3$, 4 °C) δ 202.7 (s; C18), 178.8 (s; C2), 176.5 (s; C2′), 161.5 (q, $^1J_{C,B}$ = 49.7 Hz; Ar′-C_i), 142.0 (s; C24), 137.2 (s; C3), 136.5 (s; C3′), 134.8 (s; Ar′-C_o), 133.6 (s; C23 and C23′), 131.4, 131.2, 130.9 (s; 4C; C4, C4′, C16 and C16′), 129.7 (s; C12 or C8), 129.6 (s, 2C; (C12′ or C8′) and (C12 or C8)), 129.2 (s; C8′ or C12′), 128.8 (q, $^2J_{C,F}$ = 27.0 Hz; Ar′-C_m), 128.7, 128.5, 128.3, 127.6 (s; 4C; C6, C6′, C14 and C14′), 127.2 (s; C10), 127.0 (s; C7 or C13), 126.5 (s, 4C; C10′, C7′, C14′ and (C13 or C7)), 124.2 (q, $^1J_{C,F}$ = 272.7 Hz; CF_3), 121.18 (s; C9 or C9′ or C11 or C11′), 120.94 (s; C15), 120.88 (s; C15′ or C5′), 120.7, 120.6, 120.3 (s, 3C; C9 and/or C9′ and/or C11 and/or C11′), 120.0 (s; C5), 119.7 (s; C5′ or C15′), 117.6 (s; Ar′-C_p), 115.7 (s; C21), 107.2 (br; C22 and C22′), 54.8 (s; C20), 41.0 (s; C19), 29.0 (s; C17), 20.9 (s; C25), 20.3 (s; C1), 20.0 (s; C1′). Anal. Calcd for $C_{75}H_{49}F_{24}N_2OBPd$ (1567.40): C, 57.47; H, 3.15; N, 1.79. Found: C, 57.60; H, 3.22; N, 1.91.

*Intramolecular Structure of Complex **4g** Determined by NMR Experiments.* The assignment of the ^{1}H resonances of the allyl fragment of **4g** was made on the basis of the dipolar and scalar interactions detected in the ^{1}H-NOESY and ^{1}H-COSY spectra, respectively, and confirmed by previously reported studies.[2d] The starting point was H17, the aliphatic signals integrating for three protons at 1.33 ppm ,which shows long-range correlation with the C═O singlets at 202.7 (C18) ppm in the ^{1}H–^{13}C HMBC spectrum. The remaining resonances were individuated following the interactions H17–H19a/H19b, H19a–H19b, H19a/H19b–H20, H20–H22/H22′, H22/H22′–H23/H23′ ,and H23/H23′–H25. In the aromatic region of the ^{1}H NMR spectrum, the only two singlets were ascribable to H10 and H10′ protons. Due to the NOE interactions of H17 with H10 and of H25 with H10′, it was possible to discriminate between the two signals, and so, the halves of the nitrogen ligand (*n* and *n*′) were differentiated. The overlap of most aromatic resonances makes difficult the assignment of other signals starting from H10, H10′ and following the scalar or dipolar interactions. Despite this, the following assignments were made: (i) H8′ was identified thanks to its NOE contacts with both H10′ and H25; (ii) H12′ was assigned due to its interactions with H10′, H22/H22′, and H23/H23′; (iii) H15′ was defined from its NOE contact with H22/H22′; (iv) H8 and H12 were assigned on the base of their interactions with H10 and H17; (v) H15 was assigned from the interaction with H20.

The similar intensities of the NOE interactions H1–H5, H1–H15 and of H1′–H5′, H1′–H15′ suggest the nearly perpendicular placement of the halves of the *N*-anthryl ligand with respect to the square-planar coordination plane of the complex, as observed in the solid state (Figure 2). Following the NOE connectivity, from H15′ and H15 it was possible to assign H1′ and H1 signals, of methyl groups of the DAB backbone, and consequently H5′ and H5. Both H15′–H22/H22′ and H5′–H22/H22′ contacts were detected in the ^{1}H-NOESY spectrum; however, the stronger intensity of the former confirms the rather inclined orientation of the *p*-methylstyrene ring with respect to the *n*′ half of the 9-anthryl ligand, delineating a solution structure essentially similar to that determined in the solid state by means of X-ray analysis (Figure 2). Other main observations that allow us to define the intramolecular structure of **4g** were the following: (i) a stronger intensity of the H5′–H23/H23′ contact is detected relative to the H5′–H22/H22′ contact; (ii) H25 interacts with H10′ and H8′ with approximately the same intensity; (iii) H23/H23′ preferentially interacts with H10′, H12′, and H5′; (iv) H22/H22′ preferentially interacts with H15′, H12′, and H15; (v) H20 interacts almost exclusively with H15; (vi) H19a weakly interacts with H10 and H5; (vii) H19b weakly interacts with H5; (viii) H17 interacts with H10 and, weakly, with H8 and/or H12.

dx.doi.org/10.1021/om400887x | *Organometallics* XXXX, XXX, XXX–XXX

*4.5.3. Synthesis of [Pd{C(O)CH(4-Me-C$_6$H$_4$)CH$_2$C(O)CH$_3$}((9-C$_{14}$H$_9$)$_2$DABMe$_2$)]$^+$[BAr′$_4$]$^-$ (**5g**).*

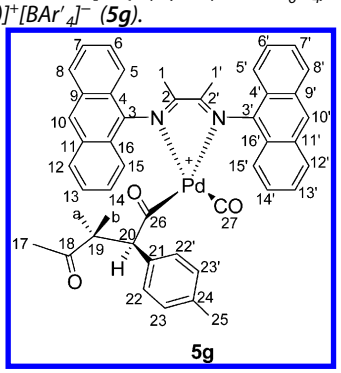

Complex **4g** (42 mg, 0.027 mmol) was dissolved in CD_2Cl_2 (0.5 mL) in an NMR tube. Carbon monoxide was bubbled through the solution for 10 min at −70 °C, resulting in the formation of an equilibrium mixture of compounds **4g** and **5g**. The equilibrium ratios appear to be strongly affected by temperature, and the highest conversion in compound **5g** (60%) was observed at −17 °C in 3 days under 1 atm of CO. ^{1}H NMR (200.13 MHz, CD_2Cl_3, −17 °C): δ 8.69 (br s, 2H; H10, H10′), 8.31−8.19 (m, 3H; H8′, H12, H12′), 8.21 (m, 1H; H8), 8.02−7.78 (m, 3H; H13, H14, H15), 8.02−7.58 (m, 21H; H5, H5′, H6, H6′, H7, H7′, H13′, H14′, H15′, Ar′-H_o, Ar′-H_p), 6.91 (d, 2H; H23 and H23′), 6.77 (d, 2H; H22 and H22′), 3.92 (dd, 1H; H20), 2.39 (s, 3H; H1 or H1′), 2.23 (m, 1H; H19b), 2.20 (s, 3H; H1′ or H1), 2.06 (s, 3H; H25), 1.61 (s, 3H; H17), 0.62 (dd, 1H; H19a). ^{13}C NMR (50.32 MHz, CD_2Cl_3, −17 °C): δ 210.1 (s; C26), 202.7 (s; C18), 169.6 (s; C27), 179.5, 173.9 (s; C2 and C2′), 161.7 (q, $^1J_{C,B}$ = 49.8 Hz; Ar′-C_i), 134.8 (s; Ar′-C_0), 131.4−120.8 (aromatic carbons and Ar′-C_m), 130.2 (br s; C23 and C23′), 129.7 (br; C22 and C22′), 124.0 (q, $^1J_{C,F}$ = 272.5 Hz; CF_3), 117.5 (s; Ar′-C_p), 60.0 (br s; C20), 44.2 (s; C19), 29.2 (s; C17), 21.4 (s; C1 or C1′), 20.7 (s; C25), 20.4 (s; C1′ or C1).

*Intramolecular Structure of Complex **5g** Determined by NMR Experiments.* The assignment of the ^{1}H resonances of the growing polymer chain of **5g** was made starting from the H20 resonance, since it is well identified at around 4 ppm, in analogy with previous results,[2d] and it is the only −C*H*− aliphatic signal in the ^{1}H NMR spectrum. The other proton resonances H19a and H19b were easily recognized, due to their direct correlation with the only −CH_2− carbon of the ^{13}C NMR spectrum. As observed in **4g**, the H22/H22′ protons (as well as H23/H23′) give a single broad doublet because of the free rotation of the *p*-methylstyrene aryl around the C20−C21 single bond. Following the dipolar interactions in the ^{1}H-NOESY spectrum and the scalar interactions in the ^{1}H−^{13}C HSQC and ^{1}H−^{13}C HMBC spectra, most of the proton and carbon resonances of the acetyl moiety were defined. Due to the presence in solution of both **4g** and **5g** and to the overlap of most aromatic signals, NOE interactions cannot be addressed to describe the intramolecular structure of **5g**. However, similarly to previous findings[2d] the preferred conformation of the growing chain was assumed to be that reported for **5g**, as confirmed from the following NMR evidence: (i) the absence of dipolar interactions involving H25 and the anthracenyl protons of the nitrogen ligand; (ii) the weak NOE contacts between H22/H22′, H23/H23′, H20 and the *N*-anthryl protons H15, H14, and H13; (iii) the interactions of H19a and H17 with H8.

*4.5.4. Synthesis of [Pd(η^3-C$_{21}$H$_{22}$O$_2$)((9-C$_{14}$H$_9$)$_2$DABMe$_2$)]$^+$[BAr′$_4$]$^-$ (**6g**).*

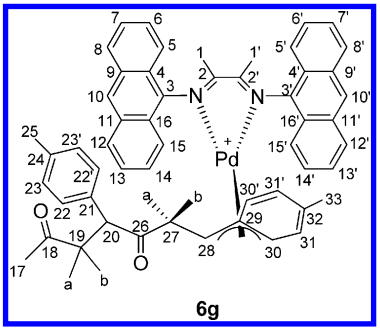

p-Methylstyrene (3.5 μL, 0.027 mmol) was added to the CD_2Cl_2 equilibrium mixture of **4g** and **5g** (40/60) in an NMR tube. Then carbon monoxide was bubbled through the solution for 5 min at −20 °C. The mixture was allowed to react for 9 days at −18 °C under 1 atm of CO. The solvent was evaporated under vacuum, and the resulting oil was washed with hexane (2 × 3 mL). The NMR analysis indicates the formation of complex **6g** as the major product (74%), together with other unidentified species. ^{1}H NMR (200.13 MHz, CD_2Cl_2, 4 °C): δ 8.68 (s, 1H; H10′), 8.32 (s, 1H; H10), 8.30 (d, $^3J_{H,H}$ = 8.8 Hz, 1H; H12′), 8.23 (d, $^3J_{H,H}$ = 8.4 Hz, 1H; H15), 8.18 (d, $^3J_{H,H}$ = 8.4 Hz, 1H; H8′), 8.07 (d, $^3J_{H,H}$ = 8.6 Hz, 1H; H15′), 7.98 (d, $^3J_{H,H}$ = 8.4 Hz, 1H; H8), 7.80 (br d, 1H; H12), 7.78−7.62 (m, 17H; H6, H13, H13′, H14, Ar′-H_o and Ar′-H_p), 7.66 (br d, 1H; H5), 7.63 (brt, 1H; H7′), 7.61 (br t, 1H; H7′), 7.56 (br t, 1H; H6′), 7.14 (d, $^3J_{H,H}$ = 8.5 Hz, 1H; H5′) 7.12 (br d, 2H; H23, H23′), 6.52 (br d, 2H; H22 and H22′), 6.19 (br, 2H; H30 and H30′), 5.83 (br, 2H; H31 and H31′), 3.16 (dd, 1H; H20), 3.08 (m, 1H; H19a), 2.50 (br s, 3H; H25), 2.45 (dd, 1H; H28), 2.41 (m, 1H; H19b), 2.21 (s, 3H; H1), 2.13 (s, 3H; H1′), 1.95 (m, 1H; H27b), 1.93 (s, 3H; H17), 0.93 (s, 3H; H33), 0.21 (dd, 1H; H27a). ^{13}C NMR (50.32 MHz, CD_2Cl_2, 4 °C) δ 207.2 (s; C18), 204.6 (s; C26), 178.7 (s; C2), 176.5 (s; C2′), 161.7 (q, $^1J_{C,B}$ = 49.8 Hz; Ar′-C_i), 141.9 (s; C32), 137.4 (s; C3), 137.3 (s; C21), 136.6 (s; C3′), 134.8 (s; Ar′-C_0), 133.5 (s; C31 and C31′), 132.7 (s; C24), 131.3, 130.9, 130.6 (s; C4, C4′, C16 and C16′), 129.6 (s; C23 and C23′), 129.5 (s; C8′), 129.4 (s; C8), 129.3 (C12′), 128.8 (q, $^2J_{C,F}$ = 27.0 Hz; Ar′-C_m), 128.7, 126.5 (s; C7, C13, C7′, C13′, C6, C14, C14′ and C10′), 128.2 (s; C12), 127.4 (s; C22, C22′, C10 and C6′), 124.2 (q, $^1J_{C,F}$ = 272.7 Hz; CF_3), 121.8 (s, C9 or C9′ or C11 or C11′), 121.1 (s; C15′), 121.0 (s; C15), 120.8 (s, C9 or C9′ or C11 or C11′), 120.4 (s, C9 or C9′ or C11 or C11′), 120.3 (s; C5), 119.9 (s; C5′), 117.5 (s; Ar′-C_p), 116.9 (s, C9 or C9′ or C11 or C11′), 55.5 (s; C28), 51.5 (s; C20), 47.6 (s; C19), 40.1 (s; C27), 29.1 (s; C17), 21.0 (s; C25), 20.7 (s; C33), 20.4 (s; C1), 20.2 (s; C1′).

*Intramolecular Structure of Complex **6g** Determined by NMR Experiments.* The analysis of the ^{1}H-NOESY spectrum of **6g** depicts the molecular structure illustrated above. Starting from H27a (a doublet of doublets at 0.21 ppm, separated from other signals in the ^{1}H NMR spectrum), the ^{1}H and ^{13}C resonances of the allyl systems were assigned on the basis of the ^{1}H−^{1}H and ^{1}H−^{13}C NMR correlations. In the aromatic region of the ^{1}H spectrum, the only singlets were ascribable to the H10 and H10′ protons. The NOE interactions of H33 with H10′ and that of H25 with H10 allow discrimination between the two signals and, then, between the halves of the 9-anthryl ligand. H10′ interacts with H8′ and H12′ and a selective NOE interaction is observed between H33 and H8′. Similarly, H10 shows dipolar interactions with H8 and H12, and the H8−H25 contact leads to assignment of the two aromatic doublets. H15′ shows a NOE interaction with the H30/H30′ resonance, while H5′ interacts preferentially with the H31/H31′ resonance, and H1′ and H1 were assigned through the interactions with H15′ and H5′ (Scheme 4). Following the NOE connectivity, from H1 it was possible to individuate H15 and H5, which were discriminated thanks to the selective H15−H28 interaction. The dipolar interactions in **6g**, involving the second *p*-methylstyrene unit and the *N*-anthryl moiety, are the same as those observed for **4g**, although with lower intensity. The position of the aryl ring of the first inserted olefin was deduced from the following observations: (i) H25 interacts with H10 and H8; (ii) H23/H23′ interact with H10 and H8 and, weakly, with H12 and H5; (iii) H22/H22′ interact with H10, H15, and H12.

4.6. General Procedures for Copolymerization Processes. *4.6.1. CO/Vinyl Arene Copolymerization in CH_2Cl_2 under 1 atm of CO.* In a typical copolymerization reaction, the Pd(II) complex (0.035 mmol) was dissolved in dichloromethane (2.8 mL) at 17 °C under a nitrogen atmosphere. The solution was transferred into a thermostated Schlenk flask equipped with a carbon monoxide gas line and a tank for the CO. Then 21 mmol of the vinyl arene (*p*-methylstyrene, 2.8 mL; styrene, 2.6 mL) was added (olefin/palladium molar ratio 600/1). The solution was allowed to react for 27 h (or 51 h) at 26 °C. The resulting gray polymer was precipitated with methanol and washed with methanol. To remove metallic palladium, the polymer was dissolved in chloroform, filtered through

dx.doi.org/10.1021/om400887x | *Organometallics* XXXX, XXX, XXX−XXX

Celite, precipitated with methanol, washed with methanol, and dried under vacuum. When mixtures of copolymer and poly(*p*-methylstyrene) were obtained from the reaction, diethyl ether was added to the mixture in order to extract the homopolymer. The resulting suspension was stirred vigorously for several hours and the ether solution was decanted off of the powder. ^{1}H and ^{13}C NMR spectroscopic data are consistent with the isolation of atactic copolymer when catalysts **2a**,**b**,**e**,**f** were used[2c,f] or predominantly isotactic polyketone when catalysts **2c**,**g** were employed.[2c]

4.6.2. CO/Vinyl Arene Copolymerization in 2,2,2-Trifluoroethanol. In a typical copolymerization reaction, the Pd(II) complex (0.035 mmol) was dissolved in 2,2,2-trifluoroethanol (2.8 mL) at 17 °C under a nitrogen atmosphere. The solution was transferred into a thermostated Schlenk flask containing 1,4-benzoquinone (19 mg, 0.175 mmol), equipped with a carbon monoxide gas line and a tank for the CO. Then 21 mmol of the vinyl arene (*p*-methylstyrene, 2.8 mL; styrene, 2.6 mL) was added (olefin/palladium molar ratio 600/1). The solution was allowed to react for 27 h at 26 °C. The resulting gray polymer was precipitated with methanol and washed with methanol. To remove metallic palladium, the polymer was dissolved in chloroform, filtered through Celite, precipitated with methanol, washed with methanol, and dried under vacuum.

4.6.3. CO/p-Methylstyrene Copolymerization in CH_2Cl_2 under 5 atm of CO. The Pd(II) complex (0.035 mmol) was dissolved in methylene chloride (2.8 mL) at 17 °C under a nitrogen atmosphere. The solution was transferred into a thermostated steel autoclave equipped with a magnetic stirring bar and a carbon monoxide gas line. Then *p*-methylstyrene (2.8 mL, 21 mmol) was introduced into the autoclave (olefin/palladium molar ratio 600/1). The nitrogen atmosphere was replaced by carbon monoxide, and the autoclave was charged with CO at 5 atm. The polymerization was allowed to run for 27 h at 26 °C. The run was terminated by venting the reactor vessel and pouring the polymerization mixture into methanol. The resulting gray polymer was washed with methanol. To remove metallic palladium, the polymer was dissolved in chloroform, filtered through Celite, precipitated with methanol, washed with methanol, and dried under vacuum.

4.7. Molecular Weight Measurements. The weight-average molecular weights (M_w) of copolymers and molecular weight distributions (PDI = M_w/M_n) were determined by gel permeation chromatography versus polystyrene standards. The analyses were recorded on a Knauer HPLC (K-501 Pump, K-2501 UV detector) with a Plgel 5 μm 10^4 Å GPC column and chloroform as solvent (flow rate 0.6 mL min^{-1}). CO/styrene samples were prepared as follows: 2 mg of the copolymer was solubilized in 120 μL of 1,1,1,3,3,3-hexafluoro-2-propanol (HFIP) and chloroform was added up to 10 mL; however, CO/*p*-methylstyrene copolymers were directly soluble in chloroform. The statistical calculations were performed with the Bruker Chromstar software program.

4.8. X-ray Crystallographic Structure Determinations for 2g and 4g. Single crystals suitable for X-ray diffraction were obtained by slow diffusion of hexane into a solution of the complex in dichloromethane with several drops of methanol at −30 °C. Diffraction data for compound **2g** and **4g** were collected on an Oxford Diffraction Xcalibur3 diffractometer equipped with a CCD area detector and Mo Kα radiation (λ = 0.71073 Å). Data collections were carried out at 150 K by means of the program Crysalis CCD,[8] and data were reduced with the program Crysalis RED.[32] The absorption correction was applied through the routine ABSPACK in the Crysalis RED program. The structures were solved with the direct methods of the SIR2004[33] package and refined by full-matrix least squares against F^2 with the program SHELX97.[34] In the crystal lattice of **2g**, additional electron density peaks were modeled as disordered acetonitrile and methanol crystallization molecules, with site occupation factor 0.5 and isotropic temperature factor (the hydrogen atoms were not introduced). In **4g**, the η^3 fragment appears disordered, except for the acetyl group. Two models for the $CH_2CH(p\text{-Me-}C_6H_4)$ moiety were found, each (a and b) with occupancy factor 0.5. In the η^3 fragment all of the atoms were refined isotropically and the hydrogen atoms were not introduced. Also for a $-CF_3$ grouping two models were found in the difference Fourier map. In this case the fluorine atoms were refined isotropically with the occupancy factor set to 0.5. In both the crystal structures all of the other non-hydrogen atoms were given anisotropic displacement parameters, and all of the other hydrogen atoms were input at calculated positions and refined by using a riding model, with isotropic thermal parameters varying in accord with those of the bound atoms. Geometrical calculations were performed by PARST97,[35] and molecular plots were produced by the program ORTEP3.[36] Crystallographic data and refinement parameters for **2g** and **4g** are reported in Table S1 in the Supporting Information.

4.9. Computational Methods. The Gaussian 09 (revision C.01)[37] package was used. Metal complexes **5c**′ and **5g**′[19] were fully optimized by using the density functional theory (DFT) method by means of Becke's three-parameter hybrid method using the LYP correlation functional.[38] The effective core potential of Hay and Wadt[39] was used for the palladium atom, and the 6-31G*[40] basis set was used for the remaining atomic species. The same model chemistry was used for the rigid potential energy surface scans performed on the postulated intermediates, resulting from the coordination of a second styrene unit to the carbonylated products **5a**′,**c**′,**f**′,**g**′. For the starting geometries of all the species modeled above, see ref 8. For the nitrogen ligands **e** and **f** the full optimization was performed at the HF-SCF level of theory, with the basis set 6-311G**.[41] The starting geometries of these latter species were based on X-ray diffraction data of analogous species. In all cases the reliability of all the found stationary points (minima on the potential energy surface) was assessed by evaluating the vibrational frequencies.

■ ASSOCIATED CONTENT

Ⓢ Supporting Information

A CIF file giving crystallographic data for **2g** and tables giving crystal data and bond distances and angles for **2g** and **4g** and Cartesian coordinates of the calculated structures. This material is available free of charge via the Internet at http://pubs.acs.org.

■ AUTHOR INFORMATION

Corresponding Author

*C.C.: tel, (+39) 0722 303312; fax, (+39) 0722 303311; e-mail, carla.carfagna@uniurb.it.

Author Contributions

The manuscript was written through contributions of all authors. All authors have given approval to the final version of the manuscript.

Notes

The authors declare no competing financial interest.

■ ACKNOWLEDGMENTS

This work was supported by the Ministero dell'Università e della Ricerca (PRIN no. 2008A7P7YJ). The CRIST (Centro di Cristallografia Strutturale), University of Florence, where the X-ray measurements were performed, is gratefully acknowledged.

■ REFERENCES

(1) Ittel, S. D.; Johnson, L.; Brookhart, M. *Chem. Rev.* **2000**, *100*, 1169−1203.

(2) (a) Bellachioma, G.; Binotti, B.; Cardaci, G.; Carfagna, C.; Macchioni, A.; Sabatini, S.; Zuccaccia, C. *Inorg. Chim. Acta* **2002**, *330*, 44−51. (b) Binotti, B.; Zuccaccia, C.; Carfagna, C.; Macchioni, A. *Chem. Commun.* **2005**, 92−94. (c) Binotti, B.; Bellachioma, G.; Cardaci, G.; Carfagna, C.; Zuccaccia, C.; Macchioni, A. *Chem. Eur. J.* **2007**, *13*, 1570−1582. (d) Carfagna, C.; Gatti, G.; Mosca, L.; Passeri, A.; Paoli, P.; Guerri, A. *Chem. Commun.* **2007**, 4540−4542. (e) Arthure, S. D.; Brookhart, M. S.; Johnson, L. K.; Killian, C. K.; McCord, E. F.; McLain, S. J. U.S. Patent 5891963, April 6, 1996. (f) Scarel, A.; Axet, M. R.; Amoroso, F.; Ragaini, F.; Elsevier, C. J.; Holuigue, A.; Carfagna, C.; Mosca, L.; Milani, B. *Organometallics* **2008**, *27*, 1486−1494.

(3) (a) Drent, E.; Budzelaar, P. H. M. *Chem. Rev.* **1996**, *96*, 663−682. (b) Bianchini, C.; Meli, A. *Coord. Chem. Rev.* **2002**, *225*, 35−66. (c) Durand, J.; Milani, B. *Coord. Chem. Rev.* **2006**, *250*, 542−560. (d) Durand, J.; Zangrando, E.; Carfagna, C.; Milani, B. *Dalton Trans.* **2008**, 2171−2182. (e) Villagra, D.; Lopez, R.; Moya, S. A.; Claver, C.; Bastero, A. *Organometallics* **2008**, *27*, 1019−1021. (f) Flipper, J.; Reek, J. N. H. *Angew. Chem., Int. Ed.* **2007**, *46*, 8590−8592. (g) Carfagna, C.; Gatti, G.; Mosca, L.; Paoli, P.; Guerri, A. *Helv. Chim. Acta* **2006**, *89*, 1660−1671. (h) Kato, J.; Taniguchi, T. Patent JP2005105470, 2005. (i) Morita, T.; Okada, S. Patent JP2005105471, 2005. (j) Durand, J.; Zangrando, E.; Stener, M.; Fronzoni, G.; Carfagna, C.; Binotti, B.; Kamer, P. C. J.; Müller, C.; Caporali, M.; van Leeuwen, P. W. N. M.; Vogt, D.; Milani, B. *Chem. Eur. J.* **2006**, *12*, 7639−7651.

(4) (a) Cheng, C.; Guironnet, D.; Barborak, J.; Brookhart, M. *J. Am. Chem. Soc.* **2011**, *133*, 9658−9661. (b) Milani, B.; Crotti, C.; Farnetti, E. *Dalton Trans.* **2008**, 4659−4663. (c) Zhang, Y.; Broekhuis, A. A.; Picchioni, F. *Macromolecules* **2009**, *42*, 1906−1912.

(5) (a) Reuter, P.; Fuhrmann, R.; Mucke, A.; Voegele, J.; Rieger, B.; Franke, R. P. *Macromol. Biosci.* **2003**, *3*, 123−130. (b) Malinova, V.; Rieger, B. *Biomacromolecules* **2006**, *7*, 2931−2936.

(6) (a) Obuah, C.; Ainooson, M. K.; Boltina, S.; Guzei, I. A.; Nozaki, K.; Darkwa, J. *Organometallics* **2013**, *32*, 980−988. (b) Meduri, A.; Cozzula, D.; D'Amora, A.; Zangrando, E.; Gladiali, S.; Milani, B. *Dalton Trans.* **2012**, *41*, 7474−7484. (c) Park, J. H.; Oh, K. H.; Kim, S. H.; Cyriac, A.; Varghese, J. K.; Hwang, M. W.; Lee, B. Y. *Angew. Chem., Int. Ed.* **2011**, *50*, 10932−10935. (d) Kageyama, T.; Ito, S.; Nozaki, K. *Chem. Asian J.* **2011**, *6*, 690−697. (e) Campos-Carrasco, A.; Estorach, C. T.; Bastero, A.; Reguero, M.; Masdeu-Bultó, A. M.; Franciò, G.; Leitner, W.; D'Amora, A.; Milani, B. *Organometallics* **2011**, *30*, 6572−6586.

(7) It is known that some aryl-substituted α-diimine ligands in square-planar complexes orient the aryl rings almost perpendicularly to the coordination plane and the ortho substituents in the apical positions. As a result, the size of the ortho substituents plays a crucial role. See: (a) Deng, L.; Woo, T. K.; Cavallo, L.; Margl, P. M.; Ziegler, T. *J. Am. Chem. Soc.* **1997**, *119*, 6177−6186. (b) Michalak, A.; Ziegler, T. *Organometallics* **2000**, *19*, 1850−1858. (c) Zhong, H. A.; Labinger, J. A.; Bercaw, J. E. *J. Am. Chem. Soc.* **2002**, *124*, 1378−1399.

(8) Carfagna, C.; Gatti, G.; Paoli, P.; Rossi, P. *Organometallics* **2009**, *28*, 3212−3217.

(9) (a) Soro, B.; Stoccoro, S.; Cinellu, M. A.; Minghetti, G.; Zucca, A.; Bastero, A.; Claver, C. *J. Organomet. Chem.* **2004**, *689*, 1521−1529. (b) Milani, B.; Scarel, A.; Zangrando, E.; Mestroni, G.; Carfagna, C.; Binotti, B. *Inorg. Chim. Acta* **2003**, *350*, 592−602. (c) Stoccoro, S.; Alesso, G.; Cinellu, M. A.; Minghetti, G.; Zucca, A.; Bastero, A.; Claver, C.; Manassero, M. *J. Organomet. Chem.* **2002**, *664*, 77−84. (d) Aeby, A.; Consiglio, G. *Inorg. Chim. Acta* **2001**, *296*, 45−51. (e) Brookhart, M.; Rix, F. C.; DeSimone, J. M.; Barborak, J. C. *J. Am. Chem. Soc.* **1992**, *114*, 5894−5895. (f) Barsacchi, M.; Consiglio, G.; Medici, L.; Petrucci, G.; Suter, U. W. *Angew. Chem., Int. Ed.* **1991**, *30*, 989−991.

(10) (a) Scarel, A.; Durand, J.; Franchi, D.; Zangrando, E.; Mestroni, G.; Carfagna, C.; Mosca, L.; Seraglia, R.; Consiglio, G.; Milani, B. *Chem. Eur. J.* **2005**, *11*, 6014−6023. (b) Binotti, B.; Carfagna, C.; Gatti, G.; Martini, D.; Mosca, L.; Pettinari, C. *Organometallics* **2003**, *22*, 1115−1123. (c) Bartolini, S.; Carfagna, C.; Musco, A. *Macromol. Rapid Commun.* **1995**, *16*, 9−14. (d) Reetz, M. T.; Haderlein, G.; Angermund, K. *J. Am. Chem. Soc.* **2000**, *122*, 996−997. (e) Brookhart, M.; Wagner, M. I.; Balavoine, G. G. A.; Haddou, H. A. *J. Am. Chem. Soc.* **1994**, *116*, 3641−3642.

(11) (a) Abu-Surrah, A. S. *Orient. J. Chem.* **2003**, *19*, 331−336. (b) Scholtz, J.; Hadi, G. A.; Thiele, K.-H.; Gorls, H.; Weimann, R.; Schumann, H.; Sieler, J. *J. Organomet. Chem.* **2001**, *626*, 243−259.

(12) Yuan, J.; Wang, F.; Xu, W.; Mei, T.; Li, J.; Yuan, B.; Song, F.; Jia, Z. *Organometallics* **2013**, *32*, 3960−3968.

(13) Rosa, V.; Avilés, T.; Aullon, G.; Covelo, B.; Lodeiro, C. *Inorg. Chem.* **2008**, *47*, 7734−7744.

(14) A linear correlation of the coordination ability of Ar-BIAN ligands toward several palladium complexes, using the corresponding aniline pK_a value, has already been reported: (a) Gasperini, M.; Ragaini, F.; Cenini, S. *Organometallics* **2002**, *21*, 2950−2957. (b) Gasperini, M.; Ragaini, F. *Organometallics* **2004**, *23*, 995−1001.

(15) (a) Schulman, S. G.; Kovi, P. J.; Torosian, G.; McVeigh, H.; Carter, D. *J. Pharm. Sci.* **1973**, *62*, 1823−1826. (b) Pankratov, A. N.; Uchaeva, I. M.; Doronin, S. Yu.; Chernova, R. K. *J. Struct. Chem.* **2001**, *42*, 739−746. (c) Rived, F.; Rosés, M.; Bosch, E. *Anal. Chim. Acta* **1998**, *374*, 309−324.

(16) (a) Milani, B.; Anzilutti, A.; Vicentini, L.; Sessanta o Santi, A.; Zangrando, E.; Geremia, S.; Mestroni, G. *Organometallics* **1997**, *16*, 5064−5075. (b) Milani, B.; Corso, G.; Mestroni, G.; Carfagna, C.; Formica, M.; Seraglia, R. *Organometallics* **2000**, *19*, 3435−3441. (c) Milani, B.; Scarel, A.; Mestroni, G.; Gladiali, S.; Taras, R.; Carfagna, C.; Mosca, L. *Organometallics* **2002**, *21*, 1323−1325. (d) Scarel, A.; Milani, B.; Zangrando, E.; Stener, M.; Furlan, S.; Fronzoni, G.; Mestroni, G.; Gladiali, S.; Carfagna, C.; Mosca, L. *Organometallics* **2004**, *23*, 5593−5605. (e) Scarel, A.; Durand, J.; Franchi, D.; Zangrando, E.; Mestroni, G.; Milani, B.; Gladiali, S.; Carfagna, C.; Binotti, B.; Bronco, S.; Gragnoli, T. *J. Organomet. Chem.* **2005**, *690*, 2106−2120.

(17) Busico, V.; Cipullo, R. *Prog. Polym. Sci.* **2001**, *26*, 443−533.

(18) (a) Koenig, J. L. *Chemical Microstructure of Polymer Chains*; Wiley: New York, 1980. (b) . Bovey, F. A; Mirau, P. A. *NMR of Polymers*; Academic Press: San Diego, CA, 1996.

(19) Complexes **5g′,c′** have the same structures as **5g,c** in Scheme 4, the only difference being the vinyl arene unit inserted (styrene instead of *p*-methylstyrene; see Scheme 4 and Figure 1). **5g′,c′** were both fully optimized with the DFT method (see Computational Methods in the Experimental Section).

(20) (a) Carfagna, C.; Gatti, G.; Martini, D.; Pettinari, C. *Organometallics* **2001**, *20*, 2175−2182. (b) Carfagna, C.; Formica, M.; Gatti, G.; Musco, A.; Pierleoni, A. *Chem. Commun.* **1998**, 1113−1114.

(21) The analytical data of the crystal structure show a distance between the phenyl ring of the η^3-allyl moiety and the N-aryl ring of 4.3 Å for **4g** (see section 2.5) and 4.6 Å for **4c**, the corresponding complex with ligand **c** (see ref 2d). Although the intermolecular π stacking interaction usually has a distance below 4 Å between the stacked rings, an intramolecular interaction with distance slightly higher than 4 Å could provide a small but still important contribution. See: Bloom, J. W. G.; Wheeler, S. E. *Angew. Chem., Int. Ed.* **2011**, *50*, 7847−7849. Grimme, S. *Angew. Chem., Int. Ed.* **2008**, *47*, 3430−3434 and references cited therein.

(22) Reddy, K. R.; Surekha, K.; Lee, G.-H.; Peng, S.-M.; Chen, J.-T.; Liu, S.-T. *Organometallics* **2001**, *20*, 1292−1299.

(23) Rix, F. C.; Brookhart, M.; White, P. S. *J. Am. Chem. Soc.* **1996**, *118*, 4746−4764.

(24) Allen, F. H. *Acta Crystallogr.* **2002**, *B58*, 380−388.

(25) The closest PF_6^- ion has been selected by considering the shortest Pd−F distance.

(26) (a) Gasperini, M.; Ragaini, F.; Gazzola, E.; Caselli, A.; Macchi, P. *Dalton Trans.* **2004**, 3376−3382. (b) Abu-Surrah, A. S.; Fawzi, R.; Steimann, M.; Rieger, B. *J. Organomet. Chem.* **1996**, *512*, 243−251. (c) Mechria, A.; Rzaiguib, M.; Bouachir, F. *Tetrahedron Lett.* **2000**, *41*, 7199−7202.

(27) According to ref 2c, the position of the counterions has been defined by the distance of each P atom from the Pd−N(1)−N(2)−C(1)−C(2) mean plane and the horizontal distance between the palladium and the intercept of the vertical distance.

(28) Tom Dieck, H.; Svoboda, M.; Grieser, T. *Z. Naturforsch., B* **1981**, *36*, 823−832.

(29) Plentz-Meneghetti, S.; Kress, J.; Peruch, F.; Lapp, A.; Duval, M.; Muller, R.; Lutz, P. J. *Polymer* **2005**, *46*, 8913−8925.

(30) Johnson, L. K.; Killian, C. M.; Brookhart, M. *J. Am. Chem. Soc.* **1995**, *117*, 6414−6415.

(31) (a) Reger, D. L.; Wright, T. D.; Little, C. A.; Lamba, J. J. S.; Smith, M. D. *Inorg. Chem.* **2001**, *40*, 3810−3814. (b) Yakelis, N. A.; Bergman, R. G. *Organometallics* **2005**, *24*, 3579−3581.

(32) *CrysAlis RED, Version 1.171.31.2*; Oxford Diffraction Ltd. (release 07-07-2006 CrysAlis171 .NET) (compiled July 10 2006, 00:11:42).
(33) Burla, M. C.; Caliandro, R.; Camalli, M.; Carrozzini, B.; Cascarano, G. L.; De Caro, L.; Giacovazzo, C.; Polidori, G.; Spagna, R. *J. Appl. Crystallogr.* **2005**, *38*, 381−388.
(34) Sheldrick, G. M. *SHELX 97*; University of Göttingen, Göttingen, Germany, 1997.
(35) Nardelli, M. *J. Appl. Crystallogr.* **1995**, *28*, 659−660.
(36) Farrugia, L. J. *J. Appl. Crystallogr.* **1997**, *30*, 565.
(37) Frisch, M. J.; Trucks, G. W.; Schlegel, H. B.; Scuseria, G. E.; Robb, M. A.; Cheeseman, J. R.; Scalmani, G.; Barone, V.; Mennucci, B.; Petersson, G. A.; Nakatsuji, H.; Caricato, M.; Li, X.; Hratchian, H. P.; Izmaylov, A. F.; Bloino, J.; Zheng, G.; Sonnenberg, J. L.; Hada, M.; Ehara, M.; Toyota, K.; Fukuda, R.; Hasegawa, J.; Ishida, M.; Nakajima, T.; Honda, Y.; Kitao, O.; Nakai, H.; Vreven, T.; Montgomery, J. A., Jr.; Peralta, J. E.; Ogliaro, F.; Bearpark, M.; Heyd, J. J.; Brothers, E.; Kudin, K. N.; Staroverov, V. N.; Keith, T.; Kobayashi, R.; Normand, J.; Raghavachari, K.; Rendell, A.; Burant, J. C.; Iyengar, S. S.; Tomasi, J.; Cossi, M.; Rega, N.; Millam, J. M.; Klene, M.; Knox, J. E.; Cross, J. B.; Bakken, V.; Adamo, C.; Jaramillo, J.; Gomperts, R.; Stratmann, R. E.; Yazyev, O.; Austin, A. J.; Cammi, R.; Pomelli, C.; Ochterski, J. W.; Martin, R. L.; Morokuma, K.; Zakrzewski, V. G.; Voth, G. A.; Salvador, P.; Dannenberg, J. J.; Dapprich, S.; Daniels, A. D.; Farkas, O.; Foresman, J. B.; Ortiz, J. V.; Cioslowski, J.; Fox, D. J. *Gaussian 09 (revision C.01)*; Gaussian, Inc., Wallingford, CT, 2010.
(38) Becke, A. D. *J. Chem. Phys.* **1993**, *98*, 5648−5652.
(39) Hay, P. J.; Wadt, W. R. *J. Chem. Phys.* **1985**, *82*, 299−310.
(40) Petersson, G. A.; Bennett, A.; Tensfeldt, T. G.; Al-Laham, M. A.; Shirlay, W. A.; Mantzaris, J. *J. Chem. Phys.* **1988**, *89*, 2193−2218.
(41) (a) McLean, A. D.; Chandler, G. S. *J. Chem. Phys.* **1980**, *72*, 5639−5648. (b) Krishnan, R.; Binkley, J. S.; Seeger, R.; Pople, J. A. *J. Chem. Phys.* **1980**, *72*, 650−654.